Journal of
Materials Chemistry C

Materials for optical, magnetic and electronic devices

## Accepted Manuscript

This article can be cited before page numbers have been issued, to do this please use: G. Kim, M. Kim, B. J. Moon, G. Moon, T. Kim, S. Ryu and S. H. Lee, *J. Mater. Chem. C*, 2026, DOI: 10.1039/D5TC04393J.

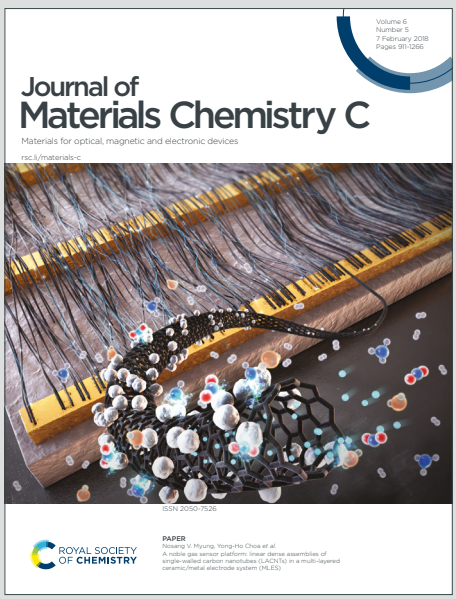




ROYAL SOCIETY OF CHEMISTRY

rsc.li/materials-c

View Article Online
DOI: 10.1039/D5TC04393J

ARTICLE



# Fluorescent Self-Reporting Theranostic Platforms for Tumour Therapy: From Cytotoxin Release Monitoring to Therapeutic Feedback Evaluation

Received 00th January 20xx,
Accepted 00th January 20xx

DOI: 10.1039/x0xx00000x

Yuning Guan,[a†] Jilei Zhao,[a†] Shaobo Hou,[a] Yingxin Sun,[a] Yalun Yao,[b] Zi Long,[b*] Jian-Liang Zhou [a*] and Chong Duan [a*]

Controlled drug release, which enables targeted drug delivery, enhances selectivity and safety, and holds broad application prospects in precision tumour therapy, is frequently limited by unpredictable cytotoxic release and variable therapeutic effects. To address this challenge, fluorescent self-reporting theranostic platforms (FSRTPs) have emerged as a promising approach, enabling real-time monitoring of drug release dynamics and therapeutic efficacy. This paper reviews fluorescent single-/dual-mode imaging-guided controlled-release therapeutics in recent years, highlighting their design rationales, imaging strategies, and biological applications. In addition, the characteristics of FSRTPs are critically compared across different therapeutic modalities from the dual perspectives of cytotoxin-release monitoring and therapeutic-feedback evaluation. A core focus is achieving high-resolution intracellular drug tracking and real-time biomarker sensing (e.g., Caspase-3) to enable prompt assessment of tumour cell apoptosis. Finally, we identify key bottlenecks in imaging depth, drug quantification, and pharmacokinetics, and propose next-generation design principles to facilitate the clinical translation of adaptive, personalized cancer therapy.

**Keywords:** Molecular imaging; Self-reported monitoring; Therapeutic feedback; Theranostic platforms; Precision cancer therapy

## 1 Introduction

Precision oncology has ushered in a transformative era of cancer therapy, shifting the paradigm from broad-spectrum intervention to highly targeted, mechanism-driven strategies[1][3]. Central to this evolution is the development of controlled-release drug-delivery systems, which are smart nanocarriers or molecular constructs capable of responding to specific endogenous stimuli (such as pH, redox, and enzymes) or exogenous stimuli (such as light, ultrasound, and magnetic fields), thereby releasing cytotoxins precisely at the tumour site[4][8]. These platforms encompass a broad therapeutic repertoire: photosensitizers (PSs)/photothermal agents (PTAs) for photodynamic therapy (PDT), photothermal therapy (PTT), enzyme-activatable prodrugs, catalytic nanozymes for chemodynamic therapy (CDT), and functional nucleic acids such as aptamers or DNAzymes[9]-[17]. Complementing these advances, a diverse array of stimulus-responsive platforms has been extensively engineered to achieve spatiotemporally controlled drug release and enhanced therapeutic specificity[18][21]. Although such switchable therapies demonstrate excellent pre-clinical efficacy, their clinical translation is limited by a critical bottleneck: the absence of a reliable correlation between external stimulus parameters (dose, exposure time, field strength) and intracellular drug-release kinetics or downstream therapeutic outcome[22][25]. This unpredictability stems from the dynamic heterogeneity of the tumour microenvironment (TME) and the lack of real-time feedback, resulting in sub-optimal synergy between dose optimization and tumour suppression. Ultimately, this

[a] School of Pharmacy, Hangzhou Normal University, Hangzhou, Zhejiang 311121, China. E-mail: cpuzhou@163.com; duanchong@hznu.edu.cn
[b] School of Civil and Architectural Engineering, Jiangxi University of Water Resources and Electric Power, Nanchang 330099, China. E-mail: 2201710194@cug.edu.cn
† These authors contributed equally to this work.

View Article Online
DOI: 10.1039/D5TC04393J





blunts the full potential of precision therapy[26][28]. Innovative approaches to bridge this gap are therefore urgently needed.

Fluorescence imaging (FLI) has emerged as a powerful tool to meet this challenge, owing to its unique ability to non-invasively visualize biological processes in real time at molecular resolution[29][30]. To bridge the gap between therapeutic action and biological response, a new class of intelligent theranostic platforms, namely fluorescent self-reporting theranostic platforms (FSRTPs), has come to the forefront of precision cancer therapy[31][32]. FSRTPs integrate therapeutic function with an intrinsic fluorescence-signalling mechanism directly coupled to key biological events, including drug release, sub-cellular trafficking, reactive oxygen species (ROS) generation, lysosomal escape, mitochondrial damage, and apoptosis induction[33]. Unlike conventional imaging-guided therapies, in which diagnosis and therapy are segregated, FSRTPs operate in a closed-loop, autonomous fashion. They continuously provide real-time optical feedback on both the therapeutic process (i.e., when and where the drug

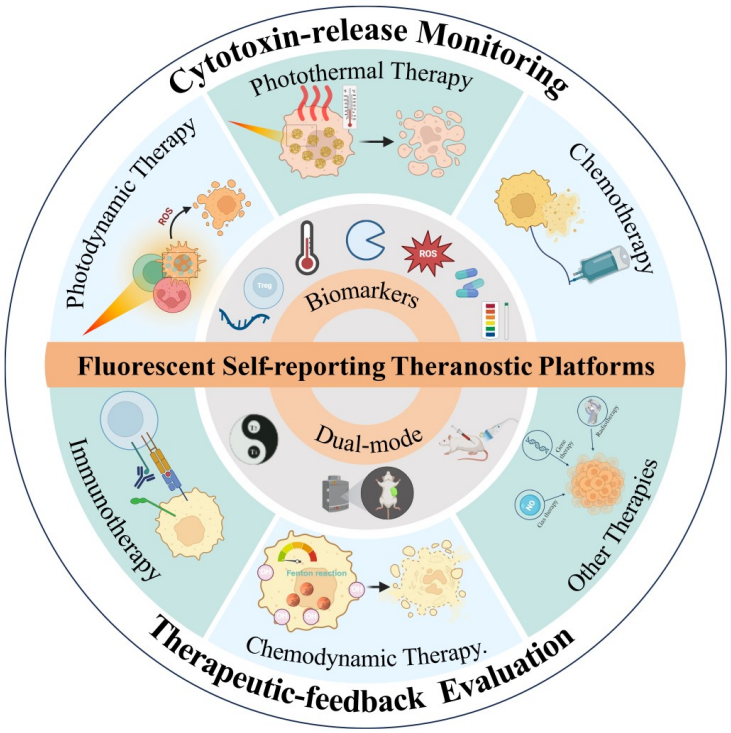


**Scheme 1**. Schematic representation of fluorescent self-reporting theranostic platforms (FSRTPs). The characteristics of FSRTPs are critically evaluated across single- and dual-modal therapeutic strategies based on their ability to monitor dynamic biomarker changes, with particular emphasis on the dual-parameter tracking of cytotoxin release and therapeutic feedback. Illustrated modalities include photothermal therapy, chemotherapy, photodynamic therapy, immunotherapy, chemodynamic therapy, and other treatment approaches.

is released) and the therapeutic outcome (i.e., cellular damage, metabolic alteration, or cell death). This dual-reporting capacity not only illuminates the molecular mechanisms underlying therapeutic pathways, markedly improving precision and clinical outcome, but also paves the way for adaptive, patient-specific intervention strategies.

Over the recent years, FSRTPs based on single- or dual-modal fluorescence imaging-guided controlled-release modalities have advanced dramatically. These systems include PDT, PTT, chemotherapy (CT), gene therapy, etc., each tailored to tumour-specific vulnerabilities[34][37]. For instance, fluorogenic prodrugs can release cytotoxic agents upon enzymatic cleavage, accompanied by fluorescence activation confirming successful release. Nanocarriers equipped with pH-responsive fluorophores enable real-time tracking of drug unloading within the acidic TME[32],[38][39]. Dual-modal systems further enhance diagnostic accuracy by integrating fluorescence with other imaging techniques (e.g., magnetic resonance imaging (MRI) or photoacoustic imaging (PAI)), offering complementary anatomical or functional information[40][42]. Nevertheless, the field still lacks a systematic review that critically evaluates the design principles, imaging strategies, and biological applications of FSRTPs across different therapeutic contexts. Moreover, comparative analyses of performance in monitoring cytotoxic agent release and assessing

 

therapeutic feedback remain scarce, hindering the rational design of next-generation platforms.

This paper aims to fill this gap by providing a comprehensive review of FSRTPs reported over the recent years, from the dual perspectives of monitoring cytotoxin release and evaluating therapeutic efficacy (**Scheme 1**). The review first systematically examines how fluorescence imaging enables precise monitoring of cytotoxin release across distinct treatment modalities, including PDT via ROS, PTT through heat-induced signal modulation, CT by drug-triggered fluorescence ON/OFF switching, and other emerging treatments. Then, the advantages of dual-mode imaging (e.g., MRI/FLI, PAI/FLI) for enhancing signal reliability, minimizing environmental interference, and enabling quantitative analysis are highlighted. The discussion then transitions from cytotoxin release monitoring to therapeutic efficacy evaluation. The paper elaborates on how single/dual-modality fluorescence imaging techniques can report biological responses post-treatment, such as cell apoptosis, necrosis, mitochondrial dysfunction, DNA damage, and immune activation, etc., thereby improving the precision of treatment (**Scheme 2**). Integrating these functionalities into a unified platform represents a paradigm shift in cancer therapy, advancing personalized, responsive, and highly effective therapeutic strategies. Such FSRTPs represent a major breakthrough in cancer therapy, offering unprecedented opportunities to optimize treatment regimens, improve patient outcomes, and deepen understanding of tumour biology. This comprehensive overview of the latest research progress in FSRTPs for tumours based on fluorescence imaging may help researchers and clinicians better understand the potential of this platform in precision cancer therapy and inspire further innovation in this promising field.

## 2 Monitoring Cytotoxin Release via FLI - Enhances the precision of drug release tracking

FLI has emerged as a key technology for real-time monitoring of drug delivery, offering unique advantages in visualizing cytotoxin release kinetics with outstanding spatiotemporal resolution[43][44]. This technique generates sensitive fluorescence turn-on or ratio change responses upon drug dissociation from carriers or prodrug activation, enabling real-time visual monitoring of drug release behavior at tumour sites and providing valuable evidence for evaluating delivery system efficiency and controllability[45][47]. In recent years, fluorescence-based

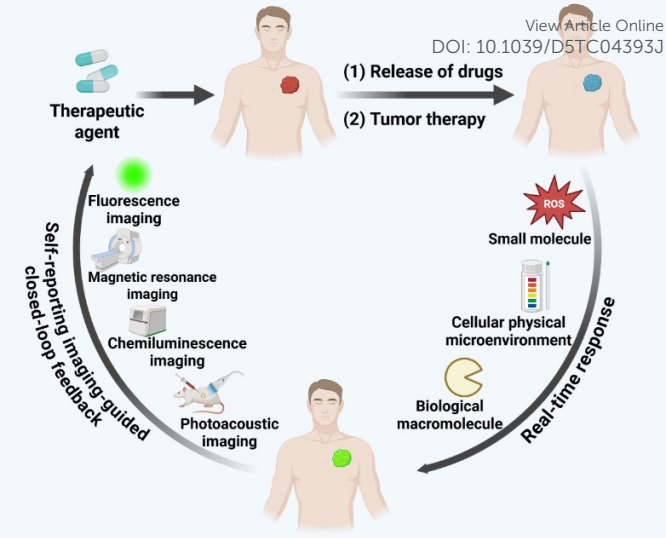


**Scheme 2**. Schematic illustration of imaging-guided closed-loop self-reporting theranostic platforms for real-time monitoring of drug release and evaluation of tumour therapy. The platforms integrate multiple imaging modalities (fluorescence, magnetic resonance, chemiluminescence, and photoacoustic imaging) and generate feedback through the monitoring of small molecules, the cellular physical microenvironment, and biological macromolecules.

release monitoring strategies have been widely integrated into various diagnosis and treatment platforms to provide real-time feedback on the onset processes of various therapeutic modalities, including chemotherapy drugs, ROS, and immunomodulators[48][51]. The following section systematically presents the diagnosis and treatment platforms for monitoring cytotoxin release using fluorescence single-modal and dual-modal imaging, and summarizes their design principles and research progress in different therapeutic modalities.

### 2.1 Monitoring via FL Single-Mode Imaging

#### 2.1.1 Monitoring in PDT

The limitations of conventional cancer therapies have prompted exploration of emerging non-invasive treatment strategies, among which PDT has emerged as one of the most promising approaches[52][54]. After decades of development, various novel PSs for PDT have been approved by the U.S. Food and Drug Administration (FDA)[55][56]. During PDT, PSs are activated by specific-wavelength light and undergo photochemical reactions with surrounding substrates (e.g., oxygen) to generate ROS, which damage cellular biomolecules and trigger anti-tumour responses. However, the operational mechanisms of PSs present limitations in clinical applications, as many current PSs lack responsiveness to specific TMEs, restricting selective cancer cell targeting and potentially causing unintended damage to nearby healthy tissues. In addition, concerns remain regarding the safety of PS

accumulation and clearance *in vivo*[32][55][57]. In this context, real-time monitoring of cancer cell viability and therapeutic response is critical for accurately assessing PDT efficacy. To address these challenges, increasing attention has been directed toward integrated theranostic platforms that can self-report ROS generation, track PS metabolism, and reflect tumour morphological changes in real time, thereby improving the precision and effectiveness of PDT. In 2019, Wang and Zhou et al. introduced UCCOFs-1, a covalent organic framework (COF)-based nano platform incorporating indocyanine green (ICG) as a singlet oxygen ($^1O_2$) reporter. This system enables efficient near-infrared (NIR) activation and in situ self-reporting PDT by generating $^1O_2$ under 980 nm NIR irradiation to activate PDT and eradicate tumour cells[58]. Concurrently, ICG degradation amplifies the upconversion luminescence (UCL) signals of UCCOFs-1 at 654 nm and 800 nm, enabling real-time *in vivo* tracking of $^1O_2$ generation loci and dosage to provide therapeutic feedback for preventing overtreatment.

To address challenges such as unintended damage to normal tissues from highly active PSs and metabolic safety concerns during *in vivo* applications, Wang et al. (2023) developed a self-immolative PS based on the BOBPY structure for precise tumour ablation. Upon light activation, the system released red-luminescent products, enabling real-time fluorescence tracking while generating cytotoxic ROS to trigger tumour cell necrosis (Figs. 1A-1B)[59]. To evaluate *in vivo* antitumour efficacy, an A549 xenograft mouse model was established, and time-dependent fluorescence accumulation at 710 nm was observed after intravenous administration of NG-cRGD. Upon 680 nm light irradiation at 24 hours post-injection, the spectra showed a decrease in 710 nm emission and a concurrent increase at 620 nm (Fig.1C), indicating in situ cleavage of the C=C bond within the TME to trigger potent phototoxicity that induces oncotic cell death. The real-time fluorescence ratio changes enabled dynamic treatment monitoring and established a theranostic platform integrating diagnostic imaging with therapeutic intervention, with the development of self-reporting organic PSs representing a promising advance in precision oncology. In the same year, Li et al. (2023) developed PTTD NPs, a multifunctional oxygen-delivery nanosystem based on metal-organic frameworks (MOFs), to alleviate tumour hypoxia via self-regulating feedback and self-amplification mechanisms[60]. This platform conducted real-time $^1O_2$ monitoring and dynamically regulated the oxygen content in the TME to optimize PDT. Under NIR irradiation, PTTD NPs suppressed mitochondrial oxygen consumption through oxidative phosphorylation (OXPHOS) pathway interference. Simultaneously, they enhanced localized oxygen enrichment to boost $^1O_2$ production, creating a synergistic "oxygen economy-PDT reinforcement" cycle. This nanosystem demonstrated remarkable efficacy in alleviating hypoxia, inhibiting tumour progression, and enabling personalized PDT through quantitative treatment monitoring. Building on these advancements, Chen et al. (2024) engineered self-reporting photodynamic nanoantibody conjugates MNB-Pyra Nbs to overcome critical PDT limitations—including off-target toxicity, hypoxia, poor accumulation, and rapid clearance[61]. The planar MNB-Pyra structure of this conjugate facilitated π-π stacking interactions that quenched fluorescence in the native state, while light-triggered ROS generation cleaved the quencher to release the PS and restore fluorescence emission, enabling real-time monitoring of both drug release dynamics and ROS production during PDT. Furthermore, nanobody (Nb) integration enhanced tumour-specific targeting, prolongs

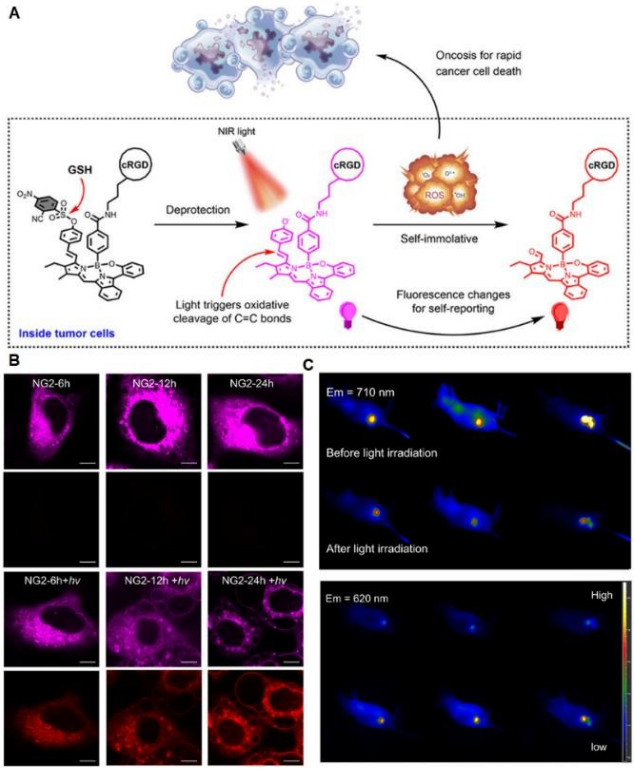


**Fig. 1** (A) Photooxidative cleavage of C=C bonds in cancer cells as an effective strategy to develop self-reporting self-imitative photosensitizers. (B) Morphological changes in A549 cells after treatment with NG2 for 6h, 12h, and 24h in the presence and absence of light illumination. (C) *In vivo* fluorescence imaging of A549-bearing mice intravenously injected with NG-cRGD after 24 h and then subjected to light irradiation. Reproduced from reference [59] with permission from the American Chemical Society.

View Article Online DOI: 10.1039/D5TC04393J



retention, thereby enabling continuous fluorescence-based tracking of therapeutic progression.

### 2.1.2 Monitoring in PTT

PTT is an efficient and non-invasive treatment modality that offers distinct advantages over conventional cancer treatment strategies[62][64]. During PTT, laser irradiation is applied to tumour regions, where PTAs convert light energy into heat, resulting in a rapid increase in local temperature. When the temperature reaches the optimal range for tumour ablation, between 42 and 45°C, irreversible damage occurs to cancer cells through protein denaturation and membrane disruption, ultimately leading to cell death[65]. Temperatures exceeding 45°C may cause damage to surrounding healthy tissues, while temperatures below 42°C may be insufficient for complete eradication of cancer cells, thereby compromising therapeutic efficacy[66]. Therefore, accurate temperature monitoring is critically important and serves as a vital measure of cytotoxicity during PTT[67][69]. Fluorescence imaging offers significant advantages for temperature monitoring during PTT due to its high sensitivity and specificity[70][71]. The development of fluorescence imaging-guided PTT platforms enables real-time tracking of thermal changes and dynamic feedback on cytotoxin release through variations in fluorescence intensity. This capability allows for timely adjustments to treatment protocols while minimizing side effects.

To monitor precise treatment, Wu et al. (2019) developed AuNBPs-DNA-TR, a reagent integrating PTT with real-time temperature monitoring to dynamically track thermal changes during PTT and provide immediate fluorescence-based feedback on cytotoxin release[72]. In this system, AuNBPs function as both photothermal converters and fluorescence quenchers for Texas Red (TR). As shown in Fig.2A, after incubation and 808 nm laser irradiation, the internalized nanoparticles produced localized hyperthermia, leading to tumour cell apoptosis. Simultaneously, temperature elevation caused conformational changes in the DNA hairpin, resulting in aggregation of AuNBPs and increased spatial separation from TR, which reduced fluorescence quenching and enabled proportional recovery of TR emission as a quantitative temperature indicator. Moreover, temperature-dependent fluorescence enhancement between 30 and 45°C confirmed the ability of AuNBPs-DNA-TR for high-resolution thermal mapping and real-time monitoring of cytotoxicity in biological settings (Figs. 2B-2E). To address the clinical challenges of overheating-induced normal tissue damage, incomplete tumour ablation, and suboptimal therapeutic outcomes in PTT, Wang et al. (2020) developed polypyrrole-rhodamine B (PPy-RB) bifunctional nanoparticles for precise treatment. These nanoparticles comprised a polypyrrole core as the PTAs and rhodamine B uniformly embedded as a temperature-sensitive probe[73]. Upon laser irradiation, PPy-RB demonstrated efficient photothermal ablation of HepG2 cells while exhibiting exceptional temperature-dependent fluorescence modulation, thereby enabling precise cytotoxic delivery monitoring and self-reporting treatment dynamics through synchronous thermal feedback.

Coincidentally, Ma et al. (2020) reported a multifunctional Nd-Ca-Si silicate glass that exhibited photothermal properties and emitted fluorescence under 808 nm laser irradiation, with intensity linearly correlated to *in situ* temperature, enabling optimal PTT treatment through temperature monitoring[74]. The Nd-Ca-Si silicate glass/sodium alginate composite hydrogel contained a bioactive silicate component that repaired thermal damage and promoted wound healing, providing self-feedback through temperature monitoring while supporting tissue repair. It is expected to be applied as an implantable medical device for PTT tumour treatment in the future. Liu et al. (2022) addressed limitations in composite probe sensitivity and deep-tissue applicability by synthesizing lanthanide-gold (LNPs-Au) nanohybrids[75]. These probes leverage rare-earth doping ($Ho^{3+}$, $Er^{3+}$, $Ce^{3+}$) to generate NIR-II emissions with depth-penetrating capabilities under

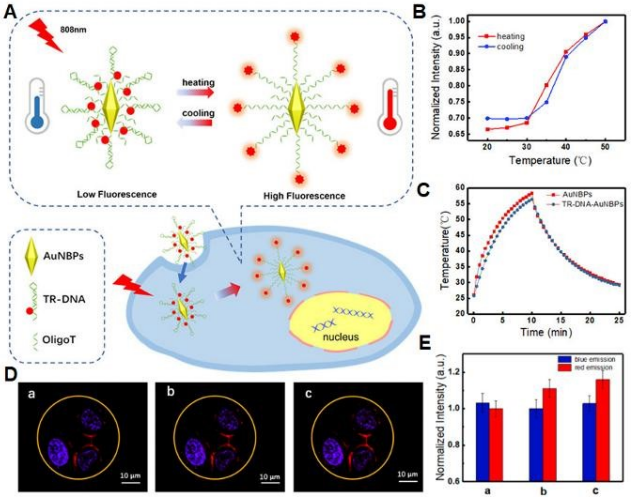


**Fig. 2** (A) Schematic illustration of AuNBPs-DNA-TR under 808 nm irradiation with thermometric function. (B) Temperature dependence of normalized FL at 610 nm. (C) Temperature variation of AuNBPs and TR-DNA-AuNBPs solution. (D) Fluorescence images of AuNBPs-DNA-TR in cells (HeLa) before (a) and after (b, c) irradiation by 808 nm laser. (E) Normalized FL of red emission and blue emission (yellow circle) in a, b, and c. Reproduced from reference [72] with permission from the American Chemical Society.

980 nm excitation. The temperature-dependent fluorescence intensity ratio (FIR) enables accurate *in situ* thermometry, mitigating overheating risks while maintaining therapeutic efficiency and highlighting the potential of ratio-based sensing for precise PTT control. Sun et al. (2023) engineered 17-RF@$Ag_2Se$ nanoparticles to achieve multimodal therapeutic capabilities, including NIR-I/II fluorescence tracking, photothermal ablation, nanothermometry, and heat shock protein inhibition[76]. Furthermore, integrin αvβ3-targeted delivery ensured tumour-specific accumulation, while $Ag_2Se$ quantum dots provide calibrated temperature feedback through temperature-sensitive emission profiles. Concomitant release of the heat shock protein inhibitor 17-AAG synergistically enhances thermal sensitivity, enabling high-resolution spatiotemporal control over PTT outcomes. This integrated system exemplifies a new frontier in self-reporting therapies by directly using diagnostic feedback to inform treatment adjustments, thereby optimizing efficacy.

### 2.1.3. Monitoring in CT

CT remains the primary treatment for most tumours today, but drug administration is frequently associated with severe toxicities and side effects[77][79], significantly restricting both the administered dosage and therapeutic efficacy[80][81]. Therefore, precise drug release and real-time monitoring at tumour sites are critical strategies to enhance drug effectiveness while minimizing toxicity[82][83]. Nonetheless, accurate monitoring of the delivery process, targeted drug release mechanisms, as well as biological distribution and metabolism of chemotherapy agents in real time remains challenging[84]. Combining non-invasive, real-time, high-resolution optical imaging with innovative anti-cancer drug-release strategies offers a powerful approach to addressing these core challenges in tumour diagnosis and therapy[85]. Biomedical researchers have designed and synthesized fluorescent small molecules that exhibited excellent performance for imaging tumour tissues and monitoring chemotherapy drug release[86][87]. The fluorescence-based small molecule drug delivery systems (DDSs) possess low toxicity coupled with strong specificity, enabling anti-cancer agents to penetrate cancer cells without harming normal cells[88][89]. Furthermore, the fluorescent moiety allows for real-time tracking of both the location and dynamics of anti-cancer drug release at subcellular levels, thus facilitating effective cancer treatment alongside cytotoxicity monitoring[39][90]. Given the numerous advantages offered by fluorescent small molecule systems as a means of delivering therapeutics, targeted treatment processes involving anti-cancer drugs have emerged as a significant research focus within contemporary cancer research and diagnostics. In 2017, Wang and Wu et al. engineered a glutathione (GSH)-triggered self-immolative prodrug (CPT-DNS-DCM) to overcome the dual challenges of controlled drug release and real-time therapeutic monitoring[91]. Subsequently, Zhang et al. (2018) developed a ROS-activatable diagnostic nanoparticle[92]. Li et al. (2020) developed ROS-sensitive mitochondrial-targeting fluorescent self-reporting polymer nanocrystals 1K-TPP and 2K-TPP to enhance ROS-responsive drug delivery[93]. These nanocrystals encapsulate doxorubicin (DOX) into homogeneous spherical micelles, triggering drug release upon exposure to 1 mM $H_2O_2$. Notably, the nanocarrier exhibits ultra-sensitive intracellular self-reporting capabilities through ratiometric fluorescence imaging. The integration of visual monitoring and therapeutic delivery has significantly advanced ROS-responsive tumour imaging technologies enable endogenous ROS stimulation to increase probes' fluorescence intensity, disrupt micelle integrity, and allow real-time visualization of drug release dynamics, while simultaneously tracking nanocrystal intracellular localization.

Polymeric micellar DDSs demonstrate potential for selective drug release in cancer cells, but face challenges such as toxicity and non-specific leakage. Shibayan Kayal et al. (2024) developed a self-reporting polymeric prodrug nanoparticle, poly-b-poly LNDA-SIPD (P3), which enables pH-responsive drug delivery and real-time release monitoring in cancer cells[94]. Using fluorescence resonance energy transfer (FRET), intracellular drug uptake and release were thus tracked. In cancerous microenvironments, P3 dissociation disrupted FRET, altering fluorescence signals to enable on-demand drug release with minimal leakage (Figs. 3A-3C). Moreover, time-dependent DOX accumulation in MCF-7 cells (1-4 h, Fig. 3D) confirmed pH-responsive release, demonstrating that P3 surpassed conventional DDSs by integrating FRET-based self-reporting for real-time monitoring, while simultaneously lowering toxicity and enhancing antitumour efficacy. This work advances the development of precision-controlled and traceable DDSs. Interestingly, Liu et al. (2025) also developed a photocaged Sanger reagent (LNDA-NBD-Sanger) for light-controlled anticancer drug delivery via FRET, utilizing photosensitive protective groups (PPGs) to regulate spatiotemporal and precise drug release[95]. FRET quenching occurred between

View Article Online
DOI: 10.1039/D5TC04393J

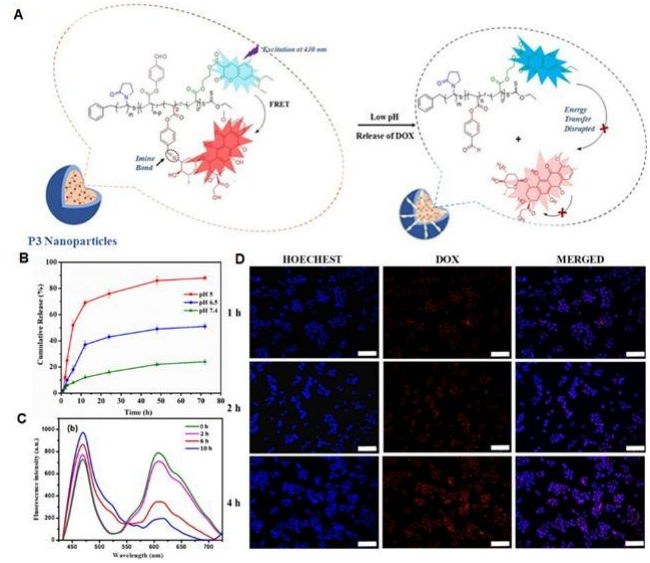


**Fig. 3** (A) Schematic representation of the energy transfer between coumarin and DOX in P3 nanoparticles. (B) pH-dependent *in vitro* DOX release profile of P3 nanoparticles. (C) Fluorescence spectra of P3 nanoparticles at different intervals of drug release. (D) Cell uptake study of P3 prodrug. Fluorescence image of P3 nanoparticles in MCF-7 cell lines over a time period of 1-4 h. The red fluorescence indicates DOX in P3 nanoparticles, and the blue fluorescence indicates the nuclei stained by HOECHST dye. Reproduced from reference [94] with permission from the American Chemical Society.

the Sanger reagent and the NBD fraction prior to 400 nm UV irradiation, and acid hydrolysis disrupted this interaction, leading to the release of the COX-2 inhibitor LNDA with anticancer activity. This innovative platform enables both real-time monitoring of drug release kinetics and self-report of treatment outcomes, advancing the development of precision oncology.

### 2.1.4. Monitoring in Other Therapies

***Gene Therapy.*** Gene therapy is a cutting-edge medical technology that treats diseases by correcting or replacing defective genes and has been widely applied in oncology[96][98]. Its efficacy depends on precise gene editing tools, such as viral vectors and lipid nanoparticles (LNPs), which show significant potential for further development. Yang et al. (2023) introduced a dual miRNA-responsive nanomedicine platform utilizing entropy-driven tetrahedral DNA circuits for gene therapy[102]. This platform detects oncogenic miRNA-155 and delivers tumour-suppressor miRNA-122 into cancer cells, triggering apoptosis while amplifying fluorescence signals through target-induced DNA conformational changes. This work represents a seminal integration of diagnosis and therapy via DNA nanotechnology, advancing clinical translation for early cancer detection and personalized treatment.

***Gene-gas Therapy.*** In addition to conventional therapeutic strategies, FSRTPs have recently emerged as innovative approaches in tumour treatment. Within this framework, gas therapy holds great potential through modulation of the physiological levels of bioactive gas molecules (e.g., nitric oxide, hydrogen sulphide, carbon monoxide, hydrogen). This modulation regulates disease-associated pathways and achieves multi-targeted therapeutic effects, demonstrating clear advantages in cardiovascular and tumour interventions[99][100]. Yang et al. (2023) pioneered gene-gas combination therapy through the development of the UV-photoresponsive cationic lipid DPNO(Zn)[101]. Its UV-triggered NO release and simultaneous fluorescence modulation overcome NO's chemical instability and short half-life within a self-reporting delivery platform. Under ultraviolet stimulation, the simultaneous delivery of NO and the TRAIL protein induced cell apoptosis, achieving synergistic anti-cancer activity. As a multifunctional material, DPNO(Zn) LNPs provide precise temporal control of treatment and integrate diagnostic capabilities through fluorescence-NO release synergy, offering transformative potential for combined cancer therapy.

***Radiotherapy.*** Radiotherapy (RT) is an effective cancer treatment method widely used in clinical practice. It utilizes high-energy radiation (including X-rays, gamma rays, and proton beams) to induce the generation of ROS through the ionization of water molecules, ultimately causing DNA damage to tumour cells to inhibit proliferation[103][104]. The role and status of RT in tumour treatment have become increasingly prominent, making it a key method for treating malignant tumours. However, its therapeutic outcome is often affected by tumour radiation resistance and dose-limiting toxicity, making it necessary to improve radiosensitivity and enable real-time monitoring of the treatment response. To this end, Ge and Su et al. (2023) developed a dual NIR region-responsive fluorescent probe (BBT-IR/Se-MN) that integrates ROS-responsive capabilities with synergistic radiosensitization for tumour ablation (Fig.4A)[105]. Under X-ray irradiation, the probe's diselenide moiety boosted ROS generation to intensify DNA damage, while its nitroimidazole group simultaneously blocked DNA repair via electron transfer, thereby yielding synergistic radiosensitization. For *in vivo* validation, longitudinal whole-body NIR-II fluorescence imaging was conducted in U87 glioblastoma-bearing mice following intravenous probe administration (Fig.4B). Notably, a strong negative correlation (Figs. 4C-4G) was established between the NIR-II fluorescence ratio and

View Article Online
DOI: 10.1039/D5TC04393J





relative tumour volume across irradiation doses, validating the probe's capacity for predictive therapeutic monitoring.

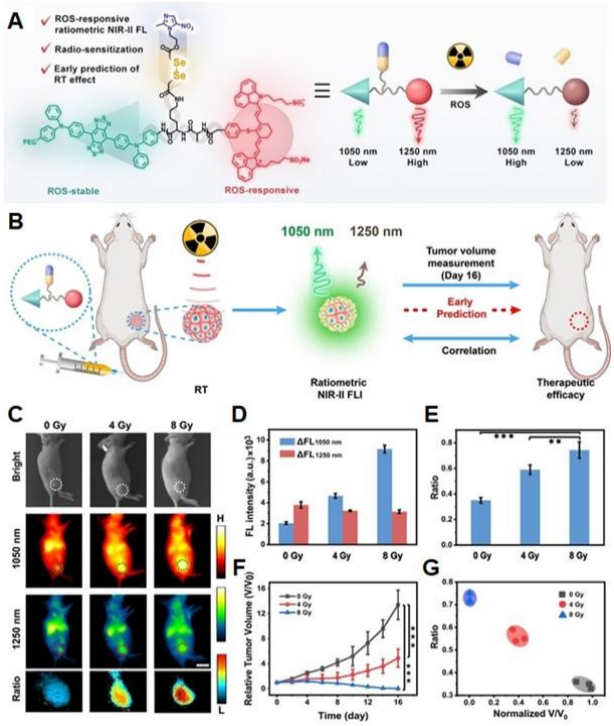


**Fig. 4** (A) Schematic illustration of ROS-responsive ratiometric NIR-II fluorescent molecule (BBT-IR/Se-MN), containing ROS-insensitive donor acceptor-donor fluorophores (BBT) and ROS-responsive cyanine dye (IR). (B) Schematic illustration of ratiometric NIR-II FL imaging in vivo. (C) NIR-II FL images of mice after different treatments. (D-E) Relative NIR-II FL signal intensity and ratios of (C). (F) Relative tumour volume changes in mice during therapy. (G) NIR-II FL intensity ratios vs the normalized relative tumour volume at day 16 after RT. Reproduced from reference [105] with permission of Wiley.

Such an innovative platform enables precise quantitative ROS assessment during radio-sensitisation and provides a strategy for enhancing RT efficacy while facilitating dose optimization and toxicity mitigation through response-guided interventions.

***Chemodynamic Therapy***. CDT has rapidly become a major treatment approach in cancer therapy in recent years, as metal ions catalyze the decomposition of overexpressed hydrogen peroxide in the TME, generating highly toxic hydroxyl radicals (·OH) through Fenton-type reactions to induce apoptosis of cancer cells[106][108]. This therapy can effectively alleviate the gradient difference between the TME and hydrogen peroxide, reducing damage to normal tissues and achieving controllable drug delivery by using biocompatible nanocarriers[109][110]. It addresses the problems of the non-specific toxicity of traditional chemotherapy and the drug resistance of RT. Compared with PDT, CDT does not rely on external energy such as oxygen and light, which makes it more useful for deep tumours with hypoxic microenvironments and poor photoactivation ability, providing a new and efficient strategy for regulating oxidative stress in cancer treatment. However, CDT also has some shortcomings, such as the low catalytic activity and limited targeting ability of commonly used metal ions. Moreover, as the treatment progresses, the low-valent metal ions are oxidized to the high-valent state, and if they cannot be replenished in time, hydroxyl radicals will not be continuously generated, resulting in failure to achieve the desired treatment effect. Therefore, real-time monitoring of the CDT process is required to improve the therapeutic efficiency.

In 2020, Ma and Yan et al. developed a nanotherapeutic system NQ-Cy@Fe&GOD to overcome the concentration-dependent limitations of Fenton reagents in generating ·OH *in vivo*, thereby enhancing treatment precision[111]. Iron oxide nanoparticles (IONPs) were employed for MRI-guided monitoring of reagent distribution to avoid healthy tissue damage from excess Fenton catalysts, while the dual-channel NQ-Cy probe enabled real-time NIR tracking of tumour-specific ·OH generation for optimal therapy (Fig. 5A-C). The system synchronized NIR-I with dosage and employed NQO1-induced NIR-II for timely monitoring of ·OH generation. Tumour-bearing mice showed pronounced NIR-I probe

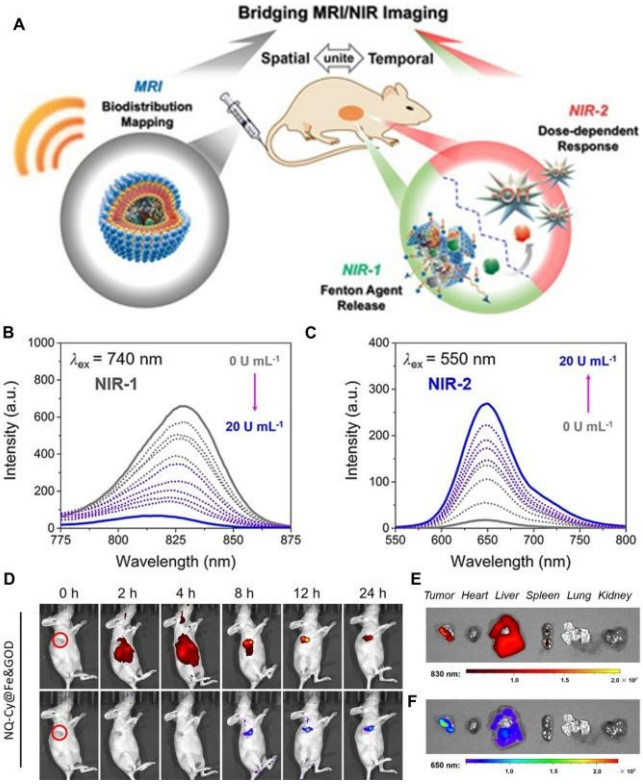


**Fig. 5** (A) Tumour-specific nanotheranostics NQ-Cy@Fe&GOD for in situ real-time reporting of Fenton-based dose-dependent ·OH generation. (B-C) Fluorescence spectra (B, $\lambda_{ex}$=740 nm; C, $\lambda_{ex}$=550 nm) of NQ-Cy (2 μm) to various

 

View Article Online
DOI: 10.1039/D5TC04393J

concentrations of NQO1 enzyme (0–20 U) and NADH in PBS at 37 °C. (D) Dual-channel NIR fluorescence imaging of NQ-Cy@Fe&GOD for in vivo monitoring after intravenous injection. (E-F) Ex vivo NIR fluorescence imaging of excised organs at 24h after intravenous injection of NQ-Cy@Fe&GOD. Reproduced from reference [111] with permission of Wiley.

accumulation at the tumour 8 h post-injection and strong NIR-II fluorescence driven by overexpressed NQO1. In contrast, non-tumour tissues remained nearly dark (Fig. 5D-F). By providing real-time visualization of tumour-targeted accumulation and response, these dual channels introduced a self-reporting, concentration-modulated CDT strategy. This approach integrated diagnostic imaging with dynamic monitoring, enabling adaptive, precision cancer care.

To address the limitations of conventional CDT reagents (complex synthesis, ROS probe consumption, restricted ·OH efficacy), Yu et al. (2024) developed Fc-CD-AuNCs, a supramolecular nanomedicine with ·OH self-monitoring ability for tumour ablation[112]. The electron-donating Fc moiety quenched the NIR-II fluorescence of CD-AuNCs via photoinduced electron transfer (PET). Upon tumour cell internalization, Fc underwent a Fenton reaction with intracellular $H_2O_2$, generating $Fc^+$ and cytotoxic ·OH, while the released $Fc^+$ product escaped from the CD cavity and restored NIR-II fluorescence through PET inhibition. This dual-functional mechanism enables real-time *in situ* visualization of ·OH generation without consuming the therapeutic ·OH molecules, representing a transformative advancement inCDT reagent design. By establishing a self-reporting system with minimal side effects, this work provides a novel paradigm for developing smart nanotherapeutics

### 2.2. Monitoring via FL Dual-Mode Imaging

Although FSRTPs have demonstrated remarkable effectiveness in evaluating tumour therapeutic outcomes, there are still several limitations of fluorescence single-modal imaging in tumour treatment monitoring[113][115]. Firstly, despite its high sensitivity, fluorescence imaging suffers from limited optical penetration depth, causing exponential signal attenuation at deep tumour lesions and micro-metastatic sites, which compromises the acquisition of high signal-to-noise ratio three-dimensional spatial distribution information [116][117]. Secondly, fluorescence single-modal imaging is confounded by autofluorescence from endogenous biomolecules, photobleaching, and complex nonlinear dependencies between fluorescence intensity, probe concentration, and local microenvironment parameters—all of which weaken signal contrast and undermine quantitative reliability. Finally, since different biological processes rely on distinct molecular mechanisms and physicochemical signals, a single imaging modality can only capture one signal type, making simultaneous multi-dimensional information acquisition impossible.

To address these deficiencies, fluorescence-based dual-modal imaging has been introduced for real-time self-reporting in tumour therapy, offering more robust signals and advancing precision medicine[118][119]. Specifically, combining FL with MRI or PAI achieves both high spatial resolution and deep-tissue penetration, overcoming the spatial-temporal resolution trade-off inherent to single modalities. Moreover, dual-modal imaging enhances quantitative accuracy through cross-validation and self-calibration across two signal channels, mitigating interference from single-signal fluctuations, which enables concurrent monitoring of multiple biological processes, thus facilitating comprehensive tracking from drug release to therapeutic outcome[120][121]. Additionally, pairing FL-based therapeutic outcome reporting (e.g., apoptosis, enzyme activation etc.) with MRI/PAI/CL-based drug distribution tracking establishes real-time mechanistic links between treatment delivery and clinical efficacy—markedly expanding the informational and predictive capacity of self-reporting platforms[122][123]. The following section systematically presents dual-modal imaging-based theranostic platforms, delineating their design principles and research progress across diverse modalities.

***Photoacoustic/Fluorescence Imaging.*** PAI technology, leveraging the photoacoustic effect, employs short-pulse laser irradiation of tissues. Exogenous or endogenous absorbers convert light into instantaneous thermal expansion and broadband ultrasound, which are detected by an ultrasonic transducer array and reconstructed into images using time-domain delay-and-sum or frequency-domain wave-number algorithms[124][125]. By combining the high contrast of optical imaging with the deep penetration of ultrasound to achieve millimetre-resolution functional images, this technology provides tumour research with a novel molecular imaging tool[126][128]. When integrated with fluorescence imaging to construct a dual-modal platform, PAI provides functional information on physiological parameters such as blood oxygen in deep tissues, while sensitive fluorescence probes label specific molecular events[129][130]. This combination not only mitigates the limited molecular specificity of PAI but also compensates for the insufficient penetration depth of fluorescence imaging, thereby achieving

complementary multi-scale information. Building upon these advantages, researchers have explored dual-modality imaging systems for therapeutic guidance, aiming to further enhance treatment precision and safety.

To minimize collateral damage to healthy tissues while enhancing therapeutic efficacy, Zheng, Dai, and Jia et al. (2020) developed a TME-responsive $Ag_2S$-GOx@BHSNY nanosystem. In the tumour microenvironment, the nanosystem degrades to release glucose oxidase (GOx) and $Ag_2S$-BSA nanoparticles. GOx catalyzes the production of $H_2O_2$, which induces the oxidation of $Ag_2S$, liberating bactericidal $Ag^+$ ions[118]. Furthermore, Gluconic acid acidifies the microenvironment, accelerating degradation and forming a self-sustaining cycle. Notably, the system enables real-time monitoring of nanoparticle distribution and therapeutic response via NIR-II fluorescence and PAI, with signals enhancing over time in correlation with nanoparticle metabolism and degradation. In 2021, Zhang et al. proposed a dual-modality imaging-guided self-feedback tumour treatment strategy to minimize off-target damage by improving illumination spatiotemporal precision[120]. This strategy, centered on the aggregation-induced emission (AIE) probe TPCB, exploited the enhanced permeability and retention (EPR) effect for tumour-targeted enrichment. PA/FL dual-modal imaging was used to pinpoint and guide irradiation, while ROS generation and apoptosis were simultaneously tracked in real time during PDT (Figs. 6A-B). The fluorescence of zinc phthalocyanine (ZnPc) in the nanoparticles was initially suppressed by aggregation-caused quenching (ACQ) but recovered following ROS-triggered nanoparticle dissociation, thereby achieving self-monitoring. Bioluminescence imaging experiments verified that prolonged light irradiation continuously enhanced TPCB fluorescence (Figs. 6C-D), and these results were consistent *in vivo* (Fig. 6E). This work highlights the advantages of the strategy and the importance of irradiation timing, offering a new tool for personalized PDT.

***Chemiluminescence/Fluorescence Imaging***. Chemiluminescence (CL) imaging forms high-sensitivity, low-noise images without external excitation. This is achieved via an enzymatic reaction that generates excited-state intermediates. Their return to the ground state emits photons, which are detected by a charge-coupled device (CCD)[131]. This imaging technique does not require an excitation light source and has low background noise and high sensitivity[132][133]. When combined with fluorescence in a dual-modal platform, chemiluminescence provides

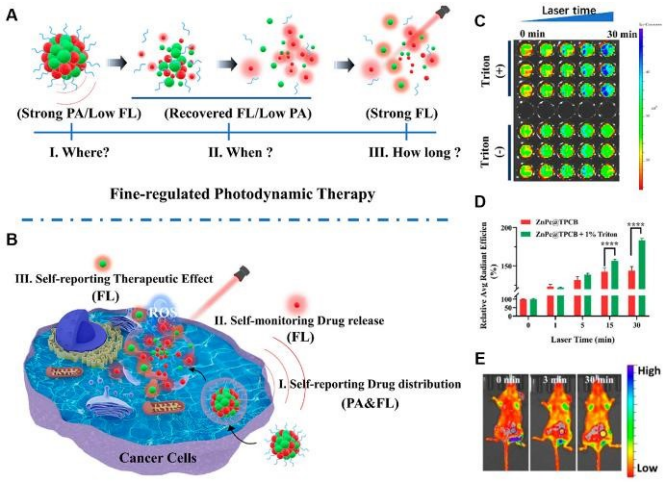


**Fig. 6** (A-B) Applications of ZnPc@TPCB NPs for fine-regulated PDT. (C) Bioluminescence imaging and (D) quantification of bioluminescence intensity of ZnPc@TPCB NPs after irradiation for different time periods with a 638 nm laser. (E) *In vivo* FL imaging of living 4T1 tumour-bearing mice after being administered with ZnPc@TPCB NPs for 24 h and irradiated for various times. Reproduced from reference [120] with permission from the American Chemical Society.

deep-tissue physiological information on gene expression and protein distribution. Meanwhile, targeted fluorescent probes enable real-time labelling of specific organelles or molecules[134][135]. This method overcomes the limitations of CL in monitoring dynamic processes and provides complementary multimodal information. To reduce ROS-induced damage to normal tissues in CDT, Lu and Zhang et al. (2020) developed a system using ultra-thin MnOx nanosheets and semiconductor polymer nanoparticles (SPNs) to improve treatment precision[121]. In this system, MnOx-generated $^1O_2$ activated NIR emission in SPNs, enhancing $^1O_2$ production for more effective therapy (Fig.7A). Leveraging the correlation between chemiluminescence-to-fluorescence (CL/FL) ratio and $^1O_2$ efficiency, ratiometric CL/FL imaging was applied for precise real-time CDT monitoring and personalized treatment (Fig.7B). The study showed that monitoring CL/FL ratios during CDT could predict $^1O_2$ output and cancer cell inhibition, offering real-time feedback for therapy optimization (Figs.7C-7E). Sulphur dioxide ($SO_2$), an emerging gaseous signalling molecule, shows therapeutic promise but remains understudied due to limited real-time monitoring. In particular, there is a lack of self-reporting $SO_2$ donors for tracking *in vivo* release, which impedes precise therapeutic evaluation. Lv's group (2025) developed an activated chemiluminescence-based self-reporting $SO_2$ donor (CL-$SO_2$D) featuring exceptional selectivity, sensitivity, and signal-to-noise ratio toward



 

View Article Online DOI: 10.1039/D5TC04393J

peroxynitrite ($ONOO^-$)[119]. This innovative donor undergoes $ONOO^-$-triggered spontaneous combustion, releasing $SO_2$ while generating reactive hydroxyl radicals that produce intense CL during electron transfer processes. Thus, CL-$SO_2$D enables *in situ* quantification of $SO_2$ delivery via CL imaging, establishing a transformative framework for creating low-background, high-sensitivity self-reporting $SO_2$ delivery systems. This advancement not only overcomes current technical barriers in $SO_2$ monitoring but also opens new avenues for investigating the dynamic roles of gaseous transmitters in TME.

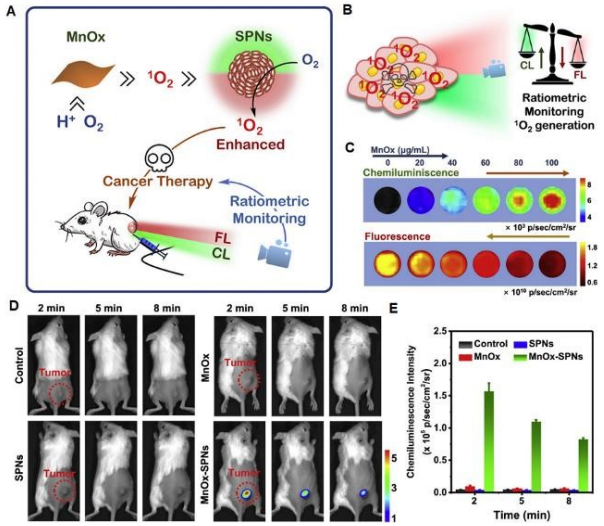


**Fig. 7** (A) Schematic illustration of pH-responsive $^1O_2$ generation and CL and ratiometric CL/FL imaging for monitoring cancer therapy. (B) Schematic of ratiometric CL/FL monitoring of dynamic therapy in vitro. (C) CL and fluorescent images of 4T1 cells treated with SPNs + different concentrations of MnOx in 96-well plates. (C-D) 4T1 tumour bearing mice i.t. injected with (1) PBS; (2) SPNs; (3) MnOx; and (4) MnOx-SPNs. (D) Representative CL images of mice. (E) Corresponding CL intensity of tumour areas from (D). Reproduced from reference [121] with permission of Elsevier.

## 3 Evaluating Therapeutic Effect via FLI-Improves the Accuracy of Treatment-Process Assessment

After the successful release and action of cytotoxins on tumour targets, evaluating the actual therapeutic effect in an accurate and timely manner is a crucial step in determining the treatment outcome and guiding subsequent intervention strategies[136]. An ideal therapeutic effect assessment should go beyond the lagging observation of tumour volume changes and focus on the early functional responses directly triggered by the treatment, such as the initiation of apoptosis, disruption of key metabolic pathways, or specific remodelling of the TME[137][138]. Taking these changes as direct readings of therapeutic effects can dynamically and prospectively reflect the treatment's efficacy. Therefore, developing monitoring strategies that can report such key physiological and pathological changes in real-time and *in situ* is essential for achieving a true closed-loop of precision treatment[139]. This section systematically elaborates on the therapeutic effect assessment strategies based on biomarker responses, with a focus on different modalities of fluorescence imaging techniques for the quantitative monitoring of the above biological changes to dynamically evaluate the efficacy of different treatment modalities. Finally, the latest applications and progress in optimizing treatment plans are summarized.

Table 1 Overview of various fluorescence imaging-guided closed-loop feedback cancer treatment platforms in monitoring cytotoxin release[a1]

| Imaging modality types | Types of therapy | Names of materials | Specific markers of self-reported monitoring | Types of imaging | Refs. |
|---|---|---|---|---|---|
| Single | PDT | UCCOFs | ROS | FL | [58] |
| Single | PDT | NG-cRGD | ROS | FL | [59] |
| Single | PDT | PTTD NPs | ROS | FL | [60] |
| Single | PDT | MNB-Pyra Nbs | ROS | FL | [61] |
| Single | PTT | AuNBPs-DNA-TR | Temperature | FL | [72] |
| Single | PTT | PPy-RB | Temperature | FL | [73] |
| Single | PTT | Nd-Ca-Si silicate glass | Temperature | FL | [74] |
| Single | PTT | LNPs-Au | Temperature | FL | [75] |
| Single | PTT | 17-RF@$Ag_2Se$ | Temperature | FL | [76] |

View Article Online
DOI: 10.1039/D5TC04393J

| | | | | | |
|---|---|---|---|---|---|
| Single | CT | 1K-TPP, 2K-TPP | Doxorubicin | FL | [93] |
| Single | CT | Poly-b-poly LNDA-SIPD | Doxorubicin | FL | [94] |
| Single | CT | LDNA-NBD-Sanger | pH | FL | [95] |
| Single | Gene therapy | Nano-theranostic platform | miRNA | FL | [102] |
| Single | Gene-gas therapy | DPNO(Zn) LNPs | RNS | FL | [101] |
| Single | RT | BBT-IR/Se-MN | ROS | FL | [105] |
| Single | CDT | NQ-Cy@Fe&GOD | ROS | FL | [111] |
| Single | CDT | Fc-CD-AuNCs | ROS | FL | [112] |
| Dual-mode | CDT | $Ag_2S$-GOx@BHSNY | pH, ROS | PA/FL | [118] |
| Dual-mode | PDT | ZnPc@TPCB NPs | ROS | PA/FL | [120] |
| Dual-mode | CDT | MnOx-SPNs | pH | CL/FL | [121] |
| Dual-mode | Gas therapy | CL-$SO_2$D | $SO_2$ | CL/FL | [119] |

[a] UCCOFs: upconversion covalent organic frameworks; NG-cRGD: initiator-N1-cyclic pentapeptide cyclo; PTPP: DSPE-SS-$PEG_{2k}$@TPP@TCPP@DPA-MOF; MNB-Pyra Nbs: MNB-Pyra and 7D12-fGly in a 1:2 tandem arrangement; AuNBPs: gold nanobipyramids; TR: Texas Red; PPy-RB: polypyrrole-rhodamine B; LNDA: lenalidomide; SIPD: self-indicating polymeric prodrug; LNPs: lipid nanoparticles; RNS: reactive nitrogen species; MN: electron-affinic nitro-compound; Fc: ferrocene; CD: cyclodextrin; AuNCs: gold nanoclusters; pH: pondus hydrogenii; BHSNY: biodegradable hollow SiO2-based nanosystem; TMZ: temozolomide; HA: hyaluronic acid; GOD: glucose oxidase; $SO_2$D: $SO_2$ donor.

### 3.1 Evaluation via FL Single-Mode Imaging

#### 3.1.1 Evaluation in PDT

In addition to the use of PDT in the self-reporting process of tumour treatment, direct monitoring of therapeutic outcomes provides a straightforward means of evaluating treatment efficacy. To overcome the limitation of conventional smart probes, Yuan and Zhang et al. (2015) developed a multifunctional probe (TPETP-SS-DEVD-TPS-cRGD) for precision treatment[140]. This probe integrates an AIE PS with a caspase-3/7-activatable apoptotic sensor, enabling tumour imaging, photodynamic ablation, and real-time therapeutic response monitoring in a single system. To address the low energy transfer efficiency of UCNPs, Zhang and Chen et al. (2021) introduced a dual surface collector system (Cy3 and Ppa with UCNPs) to significantly enhance energy transfer efficiency[141]. This system features a peptide-conjugated QSY7 quencher on the UCNP surface, enabling precise LRET-based caspase-3 biosensing through distance-dependent fluorescence quenching of Cy3. Concurrently, $Er^{3+}$ energy harvested by Ppa is efficiently transferred to dissolved oxygen, enhancing ROS generation and PDT efficacy. This work not only demonstrated the potential of UCNPs in precision medicine but also introduced a self-reporting mechanism for apoptotic biomarker monitoring. In parallel, Wang et al. (2021) developed a therapeutic PS (TPA-3Py$A^+$) to overcome the inherent limitations of single-emission PSs, which are prone to concentration- and excitation-dependent signal interference[142]. The D-π-A structured TPA-3Py$A^+$ exhibits robust $^1O_2$ production in aqueous solutions and dual-color fluorescence emission. Upon continuous irradiation, cell death dynamics are reflected by shifts in emission color, intensity and localization, with enhanced green fluorescence selectively accumulating in the nuclei of dead cells. This unique optical signature enables discrimination between live and dead cells and facilitates real-time PDT monitoring while eliminating interference from monochromatic intensity fluctuations. Collectively, these advancements highlight the transformative potential of self-reporting PSs in precision oncology and provide a foundation for the development of next-generation phototherapeutic modalities.

In 2023, Peng et al. developed a self-reporting PS based on the BOPHY structure (TPA-BPY) for monitoring

cell viability, which overcomes the stability limitations associated with high photostability requirements in NIR self-reporting PSs[143]. By employing triphenylamine as the donor to construct a donor-acceptor-donor (D-A-D) configuration, high polarity sensitivity and intramolecular charge transfer (ICT) effects are achieved, thereby improving ROS generation efficiency and therapeutic outcomes. The polarity-sensitive fluorescence intensity of TPA-BPY exhibits a linear correlation with cellular polarity, enabling *in situ* monitoring of treatment efficacy through fluorescence variations and real-time PDT feedback. Xu et al. (2024) also designed a water-soluble intelligent probe DTPAP-TBZ-I@BSA optimized for short-wave infrared applications based on the D-A-D framework[144]. Enhanced interactions between charged moieties and biomolecules, coupled with van der Waals forces, amplify both fluorescence emission and ROS production. Dynamically labeling organelles according to cellular state, this probe tracks their cytoplasm-to-nucleus migration and delivers treatment-outcome reports while demonstrating potent tumour-suppression capability. In the same year, Zhang et al. developed a series of tumour-specific PDT sensitizers (IVP-F, IVP-Cl, IVP-Br) with self-reporting functions for highly selective cancer cell ablation[145]. Among these, IVP-Br uniquely distinguishes and eradicates cancer cells by exploiting elevated mitochondrial membrane potentials and plasma membrane permeability in malignant cells, allowing preferential accumulation in mitochondrial and nucleolar compartments while excluding normal cells. The staining pattern shifts with decreasing membrane potential, enabling real-time visualization of treatment progression and self-reported therapeutic assessment.

To optimize dose-to-light interval (DLI) timing in PDT and mitigate PS-dependent poor therapeutic efficacy and adverse effects, Bian et al. (2025) engineered a photodynamic therapeutic nanoagent (CDPN) capable of real-time cell death monitoring[146]. During PDT, CDPN generates ROS to induce tumour cell apoptosis, resulting in potassium efflux and increased extracellular potassium concentration ($[K^+]_{ex}$), which allows real-time self-feedback on treatment through monitoring of $[K^+]_{ex}$ (Fig.8A). To validate the capability of CDPN for dynamic tumour apoptosis visualization, $[K^+]_{ex}$-based fluorescence imaging was conducted under different dosages and incubation conditions, as shown in Figs. 8B-8F. Without laser irradiation, CDPN exhibited low cytotoxicity toward 4T1 cells, maintaining over 85% viability after 24 hours. Furthermore, CDPN employed $[K^+]_{ex}$ as a real-time PDT biomarker to enable autonomous treatment assessment, optimize DLI, boost therapeutic efficacy, and advance precision medicine (Fig.8G). Establishing the dynamic relationship between the PDT process and change in mitochondrial viscosity is of great significance to promote the integration of tumour diagnosis and treatment. Therefore, Yin et al. designed a D-π-A type organic small molecule PS (named TKC) with good reactive oxygen generation efficiency. This could be specifically enriched in the mitochondrial membrane via electrostatic interactions, enabling real-time *in situ* imaging of mitochondrial viscosity and accurate differentiation between normal and cancer cells[147]. With its self-reporting function, TKC simultaneously tracks mitochondrial depolarization and viscosity changes during apoptosis while providing real-time feedback on PDT efficacy. In addition, TKC exhibits high phototoxicity in cells and achieves both tumour imaging and anti-tumour therapy in tumour-bearing mouse models. This study provides a feasible strategy for the development of PSs with mitochondrial targeting and self-monitoring abilities.

### 3.1.2 Evaluation in PTT

In addition to self-reporting of cytotoxin release, evaluation of PTT efficacy has also been reported in recent years. To address the clinical challenge of decoupling treatment delivery from real-time efficacy evaluation, Wang and Du et al. (2020) developed a small-molecule NIR nanoparticle probe (Cy-CBT-NP) for instantaneous PTT efficiency assessment[148]. This innovative system is internalized by tumour cells and activated by laser irradiation, triggering caspase-3-mediated apoptosis. Caspase-3 cleavage of the DEVD-Lys amide bond within the nanoparticle structure disrupts fluorescence quenching, producing a "turn-on" NIR signal that is quantitatively correlated with both treatment efficacy and apoptotic activity. This self-reporting mechanism allows adjustments of therapeutic strategies in real time, advancing personalized medicine paradigms. Subsequently, Liu et al. (2021) introduced a ratiometric fluorescence sensing platform UCNP@PDA@Cy3-pep that monitors caspase-3 activity to evaluate PTT-chemotherapy synergism[149]. Caspase-3-mediated cleavage of the DEVD recognition sequence disrupts FRET between the peptide and Cy3 dye, restoring Cy3 fluorescence for apoptosis visualization. In the same year, Long and Hu et al. (2021) developed a NIR-II photothermal nanosystem with self-feedback capabilities, integrating AIE fluorophores and $RR_9$

peptide-modified nanoparticles ($DTPRR_9$) for PTT precision therapy[150]. Such $DTPRR_9$ targets the cell membrane, and upon

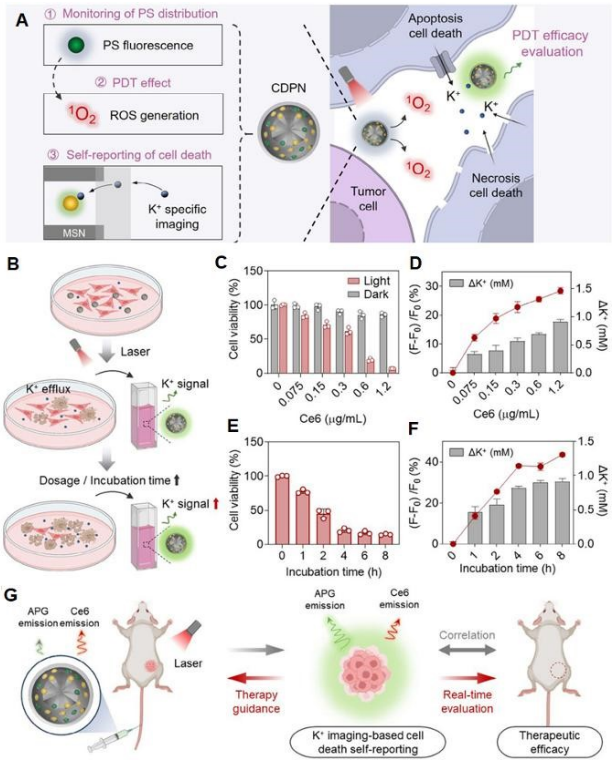


**Fig. 8** (A） CDPNs combine PDT effects with visualization of photosensitizer (PS) accumulation and self-reporting of cell death. (B) Schematic illustration of CDPN-based extracellular $K^+$ fluorescence imaging for indicating cell death under different PDT conditions. (C) Cell viability of 4T1 cells incubated with different concentrations of CDPNs with or without 671 nm irradiation. (D) Increase in extracellular [$K^+$] fluorescence signals (red line) after PDT treatment with varying CDPN concentrations and the corresponding [$K^+$] quantification using ICP-OES. (E) Cell viability of 4T1 cells under different incubation times with CDPNs with 671 nm irradiation. (F) Increase in extracellular $K^+$ fluorescence signals (red line) after PDT treatment with varying CDPN incubation times and the corresponding [$K^+$] quantification using ICP-OES. Reproduced from reference [146] with permission of the Creative Commons CC-BY.

irradiation with a 1064 nm laser, induces a localized thermal effect that causes tumour cell membrane rupture and subsequent nuclear translocation of AIE fluorescence, providing real-time visual feedback on treatment effectiveness. This system enables precise parameter optimization, minimizes normal tissue damage, and establishes the foundation for adaptive PTT strategies that effectively balance therapeutic efficacy and safety.

Intracellular viscosity, a critical parameter of the TME, is closely related to cellular processes, and its abnormal increase often indicates cell death. To address the lack of viscosity-responsive fluorophores for early cancer treatment evaluation and disease monitoring, Li et al. (2022) developed LET-1052, a pH/viscosity-activatable polymethylene blue dye for TME-responsive NIR-II PTT[151]. The therapeutic efficacy of LET-1052 was systematically evaluated through a combination of *in vivo* dose escalation studies and multimodal imaging approaches. *In vivo* experiments with escalating doses of LET-1052 demonstrated clear, dose-dependent therapeutic effects. The treatment response was further assessed via viscosity-dependent mechanisms, as shown in Figs. 9A-9B, providing insights into the microenvironmental changes during therapy. NIR-I fluorescence imaging revealed progressively expanded areas of tumour cell death and increased fluorescence intensities with higher doses (Figs. 9C-9D), reflecting enhanced therapeutic activity. Notably, a strong positive correlation was observed between NIR-I fluorescence intensity and the tumour inhibition rate (Fig. 9E), establishing a non-invasive biomarker for real-time, predictive assessment of treatment response. This integrated approach enables both precise monitoring and optimization of therapeutic outcomes.

### 3.1.3 Evaluation in CT

Assessing the effectiveness of chemotherapy in real time through integrated diagnosis and treatment platforms can mitigate the limitations imposed by its broad-spectrum nature, thereby optimizing treatment plans and enabling personalized adjustments in a timely manner[152]. In recent years, related research has been conducted on the efficacy evaluation of chemotherapy based on FSRTPs. Based on the advantages of graphene oxide (GO) in tumour targeting, drug delivery, and minimizing off-target effects, Tian and Luo et al. (2016) developed a multifunctional platform integrating targeted drug delivery with treatment monitoring[153]. In 2017, Luo et al. synthesized the

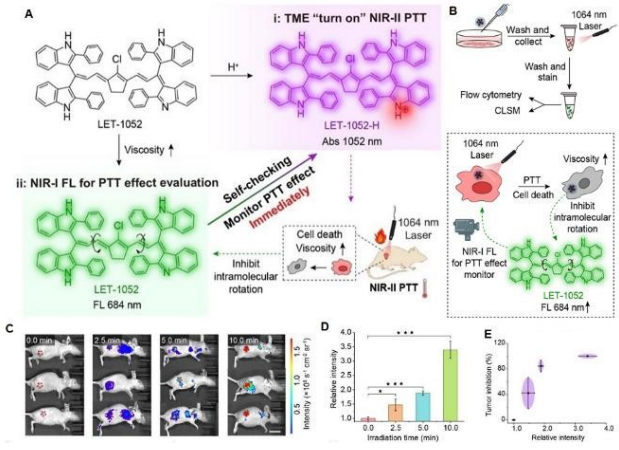


**Fig. 9** (A) Illustration of an instant evaluation strategy of therapeutic efficacy via dual pH/viscosity activatable NIR-II molecule LET-1052 by self-checking strategy. (B) Scheme of the cell sample process and the corresponding illustration of the "self-checking" strategy. Confocal microscopy images. (C) In vivo NIR-I fluorescence imaging of 4T1 tumour-bearing mice after intravenous injection of LET-1052 probe with different laser irradiation times. (D) Relative NIR-I fluorescence intensity in the red circles in (C). (E) Correlation between relative NIR-I fluorescence intensity and tumour growth inhibition 14 days after different

View Article Online
DOI: 10.1039/D5TC04393J

treatments calculated from (D). Reproduced from reference [151] with permission of Wiley.

multifunctional GAI@CP nanoparticle system to overcome limitations in current theranostic platforms for complete tumour eradication[154]. Subsequently, Yang et al. (2020) developed a nanoprobe (Au-D(Dox)-P) that integrates acid-responsive drug delivery with caspase-3-activated fluorescence imaging for precise cancer therapy[155]. This system comprises an acid-sensitive DNA duplex (D) and a caspase-3-cleavable peptide (P). After cellular uptake, the I-strand in D undergoes pH-induced conformational change in the TME, releasing DOX for targeted cancer cell killing. In apoptotic cells, caspase-3 cleaves the peptide linker, releasing FAM from gold nanoparticle quenching and restoring strong fluorescence. This self-reporting mechanism allows real-time visualization of apoptosis and quantitative assessment of therapeutic efficacy, with potential for clinical application.

Traditional chemotherapy is limited by poor selectivity, systemic toxicity, and the absence of real-time monitoring. To overcome these limitations, Pei and Liu et al. (2025) designed a self-reporting ratiometric AIE-peptide nanoprobe (TPE-1(Hyd-DOX)-DEVD) for activated chemotherapy and non-invasive therapeutic monitoring[156] TPE fluorescence in the nanoprobe is initially quenched by DOX via FRET, and upon tumour cell endocytosis, lysosomal acidity triggers DOX release, inducing apoptosis and caspase-3 upregulation. Meanwhile, caspase-3 cleaves the DEVD peptide, releasing TPE-1 fragments that disrupt FRET and self-assemble into nanofibers. This process activates AIE and enhances the TPE/DOX fluorescence ratio—a real-time biomarker for prodrug activation and efficacy (Fig.10A). Dual-channel imaging of A375 cells revealed a progressive increase in the TPE/DOX ratio over 8-24 hours, reflecting apoptosis progression (Figs. 10B-10D). This ratiometric AIE probe enables precise, non-invasive chemotherapy monitoring by integrating self-reporting with activatable therapy, supporting real-time optimization and personalized treatment and improving outcomes through dynamic feedback.

### 3.1.4. Evaluation in Other Therapies

In addition to the treatment methods mentioned above, there are also relevant reports on the efficacy evaluation of other treatment approaches based on the FSRTPs.

***Radiotherapy.*** In 2020, Wang, Jiang, and Xiao et al. developed a nano-pomegranate (RNP) platform to enhance RT efficacy by addressing the limited tissue penetration of traditional nano-radiosensitizers[157]. This platform integrates therapeutic enhancement with non-invasive, real-time monitoring to improve RT outcomes by dynamically tracking treatment responses. Upon X-ray irradiation, severe genomic damage and impaired DNA repair are induced, leading to apoptosis in cancer cells. To monitor this process, a caspase-3-responsive apoptotic sensing module is incorporated into the system. This module employs a caspase-3-cleavable DEVD peptide to link fluorescein (FITC, a fluorophore) and $Au_5$ nanoparticles (a quencher). In the initial state, FITC fluorescence is effectively quenched through nanoparticle surface energy transfer (NSET). Upon activation of caspase-3 during apoptosis, the DEVD linker is specifically cleaved, releasing FITC and restoring its fluorescent signal. This fluorescence restoration provides a direct readout of caspase-3 activity, enabling real-time quantification of RT responsiveness. By coupling dynamic therapeutic monitoring with feedback-driven adjustment, the system allows for real-time optimization of radiotherapy, thereby enhancing precision and efficacy while improving overall treatment outcomes.

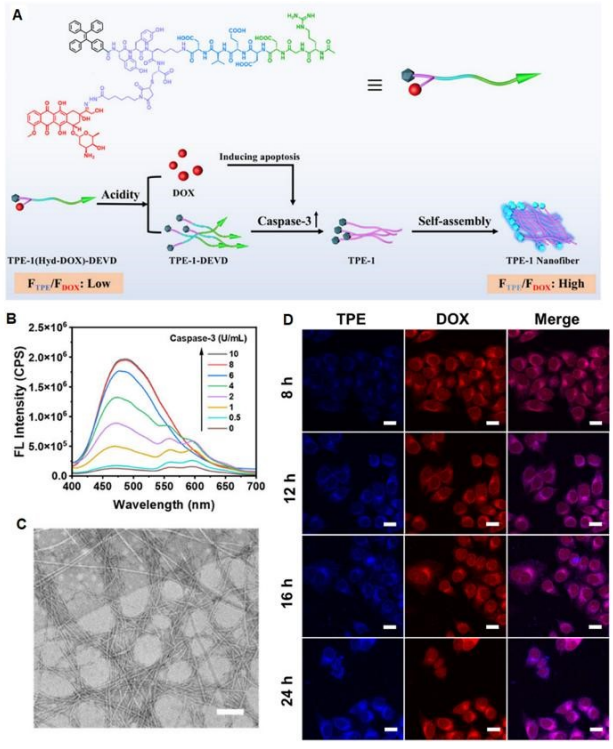


**Fig. 10** (A) Schematic illustration of the self-reporting ratiometric AIEgen-peptide nanoprobe for selective activation of DOX and real-time monitoring of therapeutic efficacy toward tumour cells. (B) Concentration dependent fluorescence spectra of TPE-1(Hyd-DOX)-DEVD in the presence of caspase-3

using 375 nm excitation. (C) TEM image of TPE-1(Hyd-DOX)-DEVD NPs following incubation with caspase-3 at pH 5.0. (D) CLSM images of A375 cells treated with TPE-1(Hyd-DOX)-DEVD NPs at various time points. Reproduced from reference [156] with permission from the American Chemical Society.

***Gas Therapy.*** Gas therapy has concurrently gained prominence in oncology due to its efficacy and favourable biosafety profile. Yue et al. (2021) engineered Au@$MnO_2$ nanomotors[158], which could induce oxidative stress by depleting GSH reserves and triggering ROS-mediated apoptosis. To realize self-reporting, FITC was conjugated to the nanomotors via Au-S bonds, and during apoptosis, caspase-3 activation cleaves the DEVEC peptides, restoring FITC fluorescence and enabling visualization of apoptosis-dependent therapeutic outcomes.

***Immunotherapy.*** Immunotherapy is a treatment approach that enhances the body's ability to recognize and eliminate tumour cells or pathogens by activating or enhancing immune function[159][160]. Unlike traditional therapies that directly attack tumour cells, it exploits the specific recognition ability of immune cells. Approaches such as immune checkpoint inhibitors (e.g., PD-1/PD-L1 antibodies) and CAR-T cell therapy disrupt immune tolerance, activate effector cells, and enhance immune memory. Thus, they achieve precise disease targeting with long-lasting response and low toxicity. Zhang et al. (2022) developed SA-CBL, a novel endoplasmic reticulum (ER)-targeted fluorescent immunogenic cell death (ICD) inducer that overcomes key limitations of conventional ICD agents—such as complex synthesis routes and heavy metal-associated toxicity[161]. SA-CBL selectively accumulates in the ER, where it triggers ROS generation and activates the unfolded protein response, ultimately leading to the release of damage-associated molecular patterns (DAMPs) and promoting dendritic cell maturation. A key feature of SA-CBL is its pH- and polarity-sensitive fluorescence (Figs. 11A-11C), which enables real-time, non-invasive monitoring of ER-targeted therapeutic effect (Figs. 11D). This self-reporting capability allows for dynamic assessment of treatment progression and efficacy. Collectively, these findings highlight SA-CBL as a transformative platform for developing organic, self-reporting ICD inducers that seamlessly integrate diagnostic imaging with immunotherapy monitoring, paving the way for precision cancer theranostics.

***Targeted Therapy.*** Organelle-targeted drug delivery, a strategy that concentrates on inducing dysfunction or structural damage of specific organelles, has emerged as a promising approach for enhanced tumor therapy[162][164]. Chen et al. (2023) developed a multifunctional peptide-conjugated probe (QRKN) that integrates therapeutic activity with self- reporting capabilities, enabling real-time monitoring of tumour treatment efficacy and prevention of

View Article Online
DOI: 10.1039/D5TC04393J

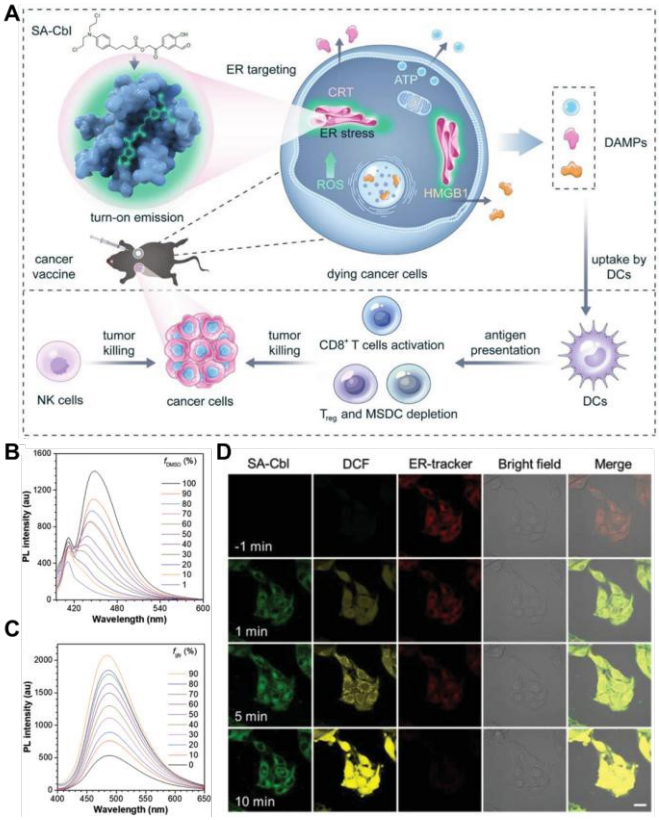


**Fig. 11** (A) Design principle of SA-Cbl as a type-II ICD inducer for cancer therapy. (B) PL spectra of SA-Cbl in DMSO/toluene solutions with different toluene fractions (C) PL spectra in PBS/glycerol solutions with different glycerol fractions. (D) CLSM images of B16F10 cells treated with SA-Cbl and co-stained with commercial ROS indicator DCFH-DA and ER-Tracker Red. Reproduced from reference [161] with permission of Wiley.

overtreatment[165]. Upon entering tumour cells, QRKN is selectively cleaved by cathepsin B (an enzyme overexpressed in cancerous environments) into two fragments, QRK and N. These fragments act synergistically to induce mitochondrial dysfunction, promote protein aggregation, and trigger apoptosis. The probe's response to intracellular changes is accompanied by the generation of fluorescence signals. As the incubation time increases, the fluorescence intensity progressively amplifies, directly correlating with rising levels of apoptosis. This intrinsic fluorescence enables dynamic, non-invasive visualization of therapeutic outcomes. Beyond tumour models, QRKN also effectively monitors cellular stress and injury progression, successfully imaging intracellular protein aggregation and apoptosis in experimental settings such as drug-induced

proteotoxic stress and simulated liver ischemia-reperfusion injury. Moreover, QRKN enables specific imaging of aggrecan, further expanding its diagnostic utility. Collectively, these features establish QRKN as a powerful theranostic agent with built-in feedback mechanisms. By integrating targeted therapy, real-time reporting, and disease-specific biomarker detection, this system provides a robust foundation for precision medicine, offering a promising strategy to reduce chemotherapy-related side effects and overcome patient resistance.

Targeted protein degradation technology (TPD) provides a precise "navigation system" for cells by designing special molecular devices that harness the ubiquitin-proteasome system (UPS) to induce the degradation of target proteins, offering a new treatment strategy for traditionally considered "undrugable" proteins[166][167] Proteolytic-targeting chimeras (PROTACs), as a representative example of TPD, employ bifunctional molecules to recruit ubiquitin ligases for ubiquitination and degradation of target proteins (POIs)[168][169]. Peptide PROTACs have attracted considerable attention due to their good biocompatibility and functional diversity. However, currently developed peptide PROTACs generally lack real-time feedback on degradation and exhibit poor pharmacokinetic stability. Therefore, Zhang (2025) et al. developed Co-SPeD, a covalent self-reporting peptide degrader that enabled real-time monitoring of targeted protein degradation while effectively suppressing tumour growth[170]. The molecular design exploited environment-sensitive fluorophore rotation: target binding rigidifies the rotor and intensifies emission, while ensuing E3 ligase recruitment and proteasomal destruction release the fluorophore, diminishing signal. These antithetical optical transitions generated real-time kinetic profiles of protein degradation. Such Co-SPeD represented a transformative theranostic platform that integrated targeted protein degradation with non-invasive, fluorescence-based monitoring, offering a powerful tool for advancing precision cancer therapy and treatment assessment. In the same year, Sun, and Wang et al. reported XZ2223, a GSH-responsive bioorthogonal theranostic probe that coupled tumour visualization with conditional protein degradation [171]. Upon disulfide reduction in the intracellular milieu, XZ2223 dually released CyNH2 for fluorescence-based tumour mapping and a tetrazine warhead for bioorthogonal prodrug activation. The latter engaged TCO-caged degraders of GSPT1 or BET proteins through rapid IEDDA chemistry, effecting localized target elimination. This imaging-guided degradation strategy, validated across cell and animal models, achieving significant therapeutic window expansion by minimizing systemic exposure—exemplifying the power of self-reporting architectures in next-generation precision oncology.

### 3.2. Evaluation via FL Dual-mode Imaging

***Photoacoustic/Fluorescence Imaging.*** Although non-invasive imaging can be evaluated in real time, it requires additional injection of probes or contrast media, which increases uncertainty and complexity. To address the above shortcomings, Wang et al. (2024) developed a dual-modality self-assessing theranostic probe (CPT-SS-DEVD-HCy) that integrates targeted cancer therapy with real-time treatment monitoring for precision oncology[122]. Upon entering tumour cells (Figs. 12A-12B), the probe is activated by the high intracellular GSH levels characteristic of the tumour microenvironment. This triggers GSH-specific reduction of the disulfide bond, leading to the release of camptothecin (CPT). CPT induces mitochondrial dysfunction and activates caspase-3, initiating apoptosis in cancer cells. The activated caspase-3 then cleaves the DEVD peptide sequence within the probe, releasing the HCy dye and generating a strong bimodal signal detectable by both FL and PA imaging. *In vitro* studies (Figs. 12C-12E) demonstrated excellent responsiveness to caspase-3 activity, characterized by a significant redshift in fluorescence emission and a notable enhancement in PA signal intensity, enabling sensitive, non-invasive monitoring of therapeutic efficacy. *In vivo* evaluation using 4T1 tumour-bearing mouse models across four treatment groups revealed that the CPT-SS-DEVD-HCy group exhibited the smallest increase in tumour volume after 14 days (Fig. 12F), confirming its potent antitumour efficacy. Importantly, the built-in feedback mechanism enabled real-time assessment of drug response through the FL/PA signals, thereby facilitating self-evaluation of treatment progression. This innovative strategy represents a significant advance in cancer theranostics, offering a powerful platform for developing intelligent, self-reporting probes that simultaneously deliver therapy and monitor outcomes, ultimately paving the way for personalized and adaptive cancer treatments.

***Magnetic Resonance/Fluorescence Imaging.*** MRI utilizes a powerful magnetic field to align the magnetic moments of hydrogen protons within the body[172]. Radiofrequency pulses excite proton resonance to produce

View Article Online
DOI: 10.1039/D5TC04393J



relaxation signals. When a gradient magnetic field is applied for spatial encoding, these signals are reconstructed into anatomical images that reveal tissue *T1*/*T2* relaxation differences[173]. When combined with fluorescence imaging to construct a dual-modal platform, MRI provides soft tissue structure information with high spatial resolution, while targeted fluorescence probes achieve molecular-level specific labelling[174][176]. This approach addresses the poor sensitivity of MRI for tiny lesions and compensates for the shortcomings of fluorescence imaging, such as the lack of anatomical reference and limited penetration depth, thereby improving the efficiency of diagnosis and treatment. The integration of diagnostic imaging with therapeutic functions has emerged as a promising strategy, inspiring the development of multifunctional nanoplatforms for cancer theranostics.

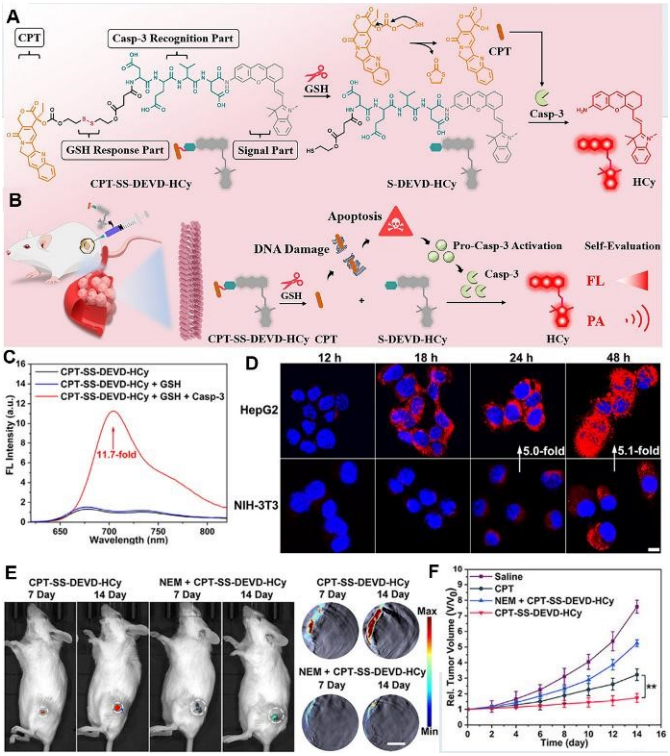


**Fig. 12** (A) Molecular transformation of CPT-SS-DEVD-HCy with GSH-controlled reduction and sequential Casp-3-controlled cleavage. (B) Schematic illustration of GSH-instructed release of CPT for tumour treatment and sequential Casp-3-controlled release of HCy for FL/PA dual-modal self-evaluation imaging of therapeutic efficacy. (C) FL spectra of 25 μM CPT-SS-DEVD-HCy with GSH or GSH and Casp-3 for 12 h. (D) Confocal FL images. (E) Relative tumour volume curves of 4T1 tumour-bearing BALB/c mice in four groups for 14 days. (F) FL images and (G) PA images at 685 nm of 4T1 tumour-bearing mice in two groups. Reproduced from reference **Error! Reference source not found.** with permission from the American Chemical Society.

To bridge the critical gap between therapeutic monitoring and clinical outcomes in catalytic therapy, Liu et al. (2024) engineered PdMn-Casp, a dual-modality theranostic platform integrating catalytic treatment with real-time self-monitoring[123]. Such system architecturally coupled Pd-Mn bimetallic nanoparticles with caspase-3-activatable NIR probes to achieve comprehensive process-to-outcome reporting. Upon accumulation in the acidic tumour microenvironment, PdMn nanoparticles underwent triggered dissolution to release $Mn^{2+}$ ions, which concurrently (i) catalyze $H_2O_2$-to-ROS conversion for cytotoxicity and (ii) generate $T_1$-MRI contrast for real-time tracking of therapeutic agent distribution and reaction kinetics. The ROS burst subsequently induced apoptotic cell death, activating executioner caspase-3 to specifically cleave the DEVD peptide linker and liberate the caged fluorophore, producing NIR fluorescence that directly reported the therapeutic efficacy. This design enabled rapid efficacy assessment: 5.8-fold fluorescence enhancement *in vitro* and significant dual-signal activation within 6 hours *in vivo*, compared to weeks required for traditional tumour volume measurements. By integrating MRI to monitor the release of therapeutic agents and fluorescence to report the treatment results, such PdMn-Casp platform realized dual-modality self-report of treatment process and efficacy, which provided a new idea for the development of intelligent diagnosis and treatment platform.

## 4 Summary and Prospects

FSRTPs represent a transformative advancement in precision cancer therapy, effectively bridging the gap between real-time monitoring and dynamic therapeutic intervention. By seamlessly integrating fluorescent probes with stimuli-responsive drug delivery systems, these platforms enable non-invasive, real-time visualization of both cytotoxin release and therapeutic efficacy, thereby establishing a closed-loop feedback system for optimized cancer management.

**Cytotoxin Release Monitoring**. In the context of cytotoxin release monitoring, fluorescence imaging, particularly through single-mode and dual-mode strategies, has emerged as a powerful tool for tracking therapeutic activation at the molecular level. Single-mode imaging, primarily based on changes in intensity, wavelength, or lifetime of fluorophores, allows precise monitoring of ROS generation in PDT, localized temperature variations in PTT, and the spatiotemporal release of chemotherapeutic agents. These systems provide critical insights into drug delivery efficiency and site-specific activation, minimizing

off-target effects. Meanwhile, dual-mode fluorescence imaging enhances

View Article Online
DOI: 10.1039/D5TC04393J

Table 2 Overview of various fluorescence imaging-guided closed-loop feedback cancer treatment platforms for assessment of treatment effect [a2]

| Imaging modality types | Types of therapy | Names of materials | Specific markers of self-reported monitoring | Types of imaging | Refs. |
|---|---|---|---|---|---|
| Single | PDT | TPETP-SS-DEVD-TPS-cRGD | Caspase-3/7 | FL | [140] |
| Single | PDT | UCNP-Cy3 | Caspase-3 | FL | [141] |
| Single | PDT | TPA-3PyA$^+$ | Subcellular localization, Color of fluorescence | FL | [142] |
| Single | PDT | TPA-BPY | Polarity | FL | [143] |
| Single | PDT | DTPAP-TBZ-I@BSA | Migration of organelles | FL | [144] |
| Single | PDT | IVP-Br | Migration of organelles | FL | [145] |
| Single | PDT | CPDN | $[K^+]_{ex}$ | FL | [146] |
| Single | PDT | TKC | Viscosity | FL | [147] |
| Single | PTT | Cy-CBT-NP | Caspase-3 | FL | [148] |
| Single | PTT | UCNP@PDA@Cy3-pep | Caspase-3 | FL | [149] |
| Single | PTT | DTPRR9 | Migration of organelles | FL | [150] |
| Single | PTT | LET-1052 | Viscosity | FL | [151] |
| Single | CT | Au-D(Dox)-P | Caspase-3 | FL | [155] |
| Single | CT | TPE-1(Hyd-DOX)-DEVD | Caspase-3 | FL | [156] |
| Single | RT | RNP | Caspase-3 | FL | [157] |
| Single | Gas Therapy | Au@$MnO_2$ | Caspase-3 | FL | [158] |
| Single | Immunotherapy | SA-Cbl | pH, Polarity | FL | [161] |
| Single | Targeted Therapy | QRKN | Protein of aggregation | FL | [165] |
| Single | Targeted Therapy | Co-SPeD | Protein | FL | [170] |
| Single | Targeted Therapy | XZ2223 | GSH | FL | [171] |
| Dual-mode | CT | CPT-SS-DEVD-HCy | Caspase-3 | PA/FL | [122] |
| Dual-mode | CDT | PdMn-Casp | Caspase-3 | MRI/FL | [123] |

[a2] UCNPs: upconversion nanoparticles; TPA: triphenylamine; PyA: cyanovinyl-pyridinium; DTPAP: donating triphenylamine TBZ: thiadiazolobenzotriazole; IVP: a series of fluorescent photosensitizers based on simple chemical structures; CDPN: cell death self-reporting photodynamic theranostic nanoagent; TKC: a mitochondria-targeted, viscosity-sensitive photosensitizer; PDA: polydopamine; $DTPRR_9$: a cell-membrane-anchored nanoassembly;; TPE: tetraphenylethylene; DEVD: a caspase-3 cleavable linker, Asp-Glu-Val-Asp; RNP: nanopomegranate platform; SA: salicylaldehyde; Cbl: chlorambucil; Co-SPeD: covalent self-reporting peptide degrader; CPT: camptothecin; SS: disulfide bond; HCy: hemicyanine.

reliability and accuracy by integrating two complementary signals (e.g., ratiometric or multi-color readouts), thereby effectively overcoming environmental interference, photobleaching, and signal fluctuation limitations. Furthermore, emerging platforms have expanded monitoring capabilities to additional cytotoxic mechanisms,

including sonodynamic therapy, ICD inducers, and targeted protein degradation, demonstrating the versatility of fluorescent reporting technology.

**Therapeutic Efficacy Assessment.** Fluorescence imaging also plays a pivotal role in evaluating therapeutic outcomes. By dynamically assessing treatment responses—such as apoptosis induction, mitochondrial dysfunction, DNA damage, and immune cell infiltration—these technologies enable early prediction of therapeutic efficacy and facilitate timely treatment adjustments. Single-mode imaging remains at the forefront for visualizing key biomarkers, including caspase-3 activity, ROS accumulation, and lysosomal damage, applicable across multiple therapeutic modalities such as PDT, PTT, and chemotherapy etc. Dual-mode imaging provides built-in reference signals to normalize background noise and biological variability, enabling quantitative analysis within complex tumor microenvironments. Notably, several advanced systems now incorporate multimodal integration—combining FL with PA, MR, or PET signals—to achieve deeper tissue penetration and higher spatial resolution.

**Current Challenges and Limitations.** Despite promising prospects, clinical translation of FSRTPs faces several fundamental challenges. The primary limitation stems from the inherent physical properties of fluorescence: restricted tissue penetration depth and high background autofluorescence, restricting current applications to superficial tumors or intraoperative navigation. To overcome this constraint, developing NIR-II fluorescent probes or integrating photoacoustic imaging should be prioritized. Additionally, transitioning from qualitative visualization to precise quantitative monitoring of drug release remains a significant challenge, as fluorescence intensity is susceptible to environmental fluctuations and probe degradation. Beyond optical performance, the long-term biosafety and complex pharmacokinetic profiles of multifunctional nanoplatforms remain inadequately characterized, necessitating rigorous evaluation of metabolic pathways and systemic toxicity. Addressing these translational barriers requires not only optimizing probe stability and signal-to-noise ratio but also establishing standardized clinical protocols.

**Future Directions.** Looking ahead, the future development of fluorescence self-reporting platforms will likely focus on several pivotal directions:

View Article Online
DOI: 10.1039/D5TC04393J

(1) Enhanced Sensitivity and Specificity: Designing next-generation probes with improved target affinity, reduced false-positive signals, and activatable responses triggered only by specific pathological cues (e.g., enzyme overexpression, pH shifts, or redox imbalances) will be crucial for clinical translation.

(2) Multifunctional Integration: Emerging platforms are likely to integrate multiple capabilities—targeted delivery, controlled release, real-time self-reporting, and immune modulation—into a single theranostic system, enabling comprehensive cancer intervention from diagnosis to therapy.

(3) Closed-Loop Feedback Systems: Integrating real-time fluorescence data with artificial intelligence (AI)-driven algorithms could enable adaptive therapy, in which treatment parameters (e.g., light dosage, drug release rate, irradiation timing) are automatically adjusted based on live imaging feedback, maximizing efficacy while minimizing damage to healthy tissues.

(4) Expansion to Diverse Cancer Types and Therapies: Although current applications predominantly target solid tumours, there is growing potential to extend these platforms to hematological malignancies, metastatic disease, and combination therapies involving immunotherapy, gene editing, or radiotherapy.

(5) Clinical Translation and Standardization: To advance from bench to bedside, rigorous validation in large animal models and early-phase clinical trials is essential. Moreover, standardization of imaging protocols, quantification metrics, and regulatory pathways will be necessary to ensure reproducibility and safety.

In conclusion, FSRTPs are redefining the paradigm of precision cancer therapy by transforming passive treatments into intelligent, responsive processes. As these technologies continue to evolve, they hold great promise for mitigating chemotherapy-related adverse effects, overcoming drug resistance, and ultimately improving patient outcomes—ushering in a new era of personalized, image-guided oncology. In the future, more efficient self-feedback diagnosis and treatment platforms are anticipated, advancing both personalized cancer treatment and precision medicine.

## Conflicts of interest

The authors declare that they have no known competing financial interests or personal relationships that could have appeared to influence the work reported in this paper.

## Data availability

Data availability is not applicable to this article as no new data were created or analyzed in this review.

## Acknowledgements

This research was supported by National Natural Science Foundation of China under Grant No. 22507035, Jiangxi Provincial Natural Science Foundation of China under Grant No. 20252BAC200227, Scientific Research Fund of Zhejiang Provincial Education Department under Grant No. Y202455881, Innovation team of Hangzhou City under Grant No. TD2024002.

## References

[1] R. L. Siegel, T. B. Kratzer, A. N. Giaquinto, H. Sung, A. Jemal, Cancer statistics, 2025, Ca- Cancer J. Clin. 75 (2025) 10-45.

[2] J. Mateo, L. Steuten, P. Aftimos, F. Andre, M. Davies, E. Garralda, J. Geissler, D. Husereau, I. Martinez-Lopez, N. Normanno, J. S. Reis-Filho, S. Stefani, D. M. Thomas, C. B. Westphalen, E. Voest, Delivering precision oncology to patients with cancer, Nat. Med. 28 (2022) 658-665.

[3] X. Wang, Y. S. Chan, K. Wong, R. Yoshitake, D. Sadava, T. W. Synold, P. Frankel, P. W. Twardowski, C. Lau, S. Chen, Mechanism-Driven and Clinically Focused Development of Botanical Foods as Multitarget Anticancer Medicine: Collective Perspectives and Insights from Preclinical Studies, IND Applications and Early-Phase Clinical Trials, Cancers (Basel) 15 (2023) 701.

[4] A. O. Elzoghby, W. M. Samy, N. A. Elgindy, Albumin-based nanoparticles as potential controlled release drug delivery systems, J. Control. Release 157 (2012) 168-182.

[5] A. S. Mikhail, R. Morhard, M. Mauda-Havakuk, M. Kassin, A. Arrichiello, B. J. Wood, Hydrogel drug delivery systems for minimally invasive local immunotherapy of cancer, Adv. Drug Deliv. Rev. 202 (2023) 115083.

[6] M. Shi, K. J. McHugh, Strategies for overcoming protein and peptide instability in biodegradable drug delivery systems, Adv. Drug Deliv. Rev. 199 (2023) 114904.

[7] J. Li, C. Fan, H. Pei, J. Shi, Q. Huang, Smart drug delivery nanocarriers with self-assembled DNA nanostructures, Adv. Mater. 25 (2013) 4386-4396.

[8] M. Kenchegowda, M. Rahamathulla, U. Hani, M. Y. Begum, S. Guruswamy, R. A. M. Osmani, M. P. Gowrav, S. Alshehri, M. M. Ghoneim, A. Alshlowi, D. V. Gowda, Smart Nanocarriers as an Emerging Platform for Cancer Therapy: A Review, Molecules 27 (2021) 146.

[9] Y. Chen, H. Li, Y. Deng, H. Sun, X. Ke, T. Ci, Near-infrared light triggered drug delivery system for higher efficacy of combined chemo-photothermal treatment, Acta Biomater. 51 (2017) 374-392.

[10] J. Shi, L. Wang, J. Zhang, R. Ma, J. Gao, Y. Liu, C. Zhang, Z. Zhang, A tumour-targeting near-infrared laser-triggered drug delivery system based on GO@Ag nanoparticles for chemo-photothermal therapy and X-ray imaging, Biomaterials 35 (2014) 5847-5861.

[11] M. Ni, W.-J. Zeng, X. Xie, Z.-L. Chen, H. Wu, C.-M. Yu, B.-W. Li, Intracellular enzyme-activatable prodrug for real-time monitoring of chlorambucil delivery and imaging, Chin. Chem. Lett. 28 (2017) 1345-1351.

[12] A. Shoaib, S. Javed, M. Tabish, M. E. Khan, M. Zaki, S. S. Alqahtani, M. H. Sultan, W. Ahsan, M. Afzal, Applications of nanomedicine-integrated phototherapeutic agents in cancer theranostics: A comprehensive review of the current state of research, Nanotechnol. Rev. 13 (2024) 1-36.

[13] X. Wu, M. Wu, J. X. Zhao, Recent development of silica nanoparticles as delivery vectors for cancer imaging and therapy, Nanomedicine 10 (2014) 297-312.

[14] S. Hou, Y.-E. Gao, X. Ma, Y. Lu, X. Li, J. Cheng, Y. Wu, P. Xue, Y. Kang, M. Guo, Z. Xu, Tumour microenvironment responsive biomimetic copper peroxide nanoreactors for drug delivery and enhanced chemodynamic therapy, Chem. Eng. J. 416 (2021) 129037.

[15] I. C. Sun, H. Y. Yoon, D. K. Lim, K. Kim, Recent Trends in In Situ Enzyme-Activatable Prodrugs for Targeted Cancer Therapy, Bioconjug. Chem. 31 (2020) 1012-1024.

[16] X. Shen, T. Li, X. Xie, Y. Feng, Z. Chen, H. Yang, C. Wu, S. Deng, Y. Liu, PLGA-Based Drug Delivery Systems for Remotely Triggered Cancer Therapeutic and Diagnostic Applications, Front. Bioeng. Biotechnol. 8 (2020) 381.

[17] J. Xiang, J. Liu, X. Liu, Q. Zhou, Z. Zhao, Y. Piao, S. Shao, Z. Zhou, J. Tang, Y. Shen, Enzymatic drug release cascade from polymeric prodrug nanoassemblies enables targeted chemotherapy, J. Control. Release 348 (2022) 444-455.

[18] C.-S. Lee, R. K. Singh, H. S. Hwang, N.-H. Lee, A. G. Kurian, J.-H. Lee, H. S. Kim, M. Lee, H.-W. Kim,

Materials-Based Nanotherapeutics for Injured and Diseased Bone, Prog. Mater. Sci. 135 (2023) 101087.

[19] R. K. Singh, A. G. Kurian, K. D. Patel, N. Mandakhbayar, N.-H. Lee, J. C. Knowles, J.-H. Lee, H.-W. Kim, Label-Free Fluorescent Mesoporous Bioglass for Drug Delivery, Optical Triple-Mode Imaging, and Photothermal/Photodynamic Synergistic Cancer Therapy, ACS Appl. Bio Mater. 3 (2020) 2218–2229.

[20] K. D. Patel, R. K. Singh, H.-W. Kim, Carbon-Based Nanomaterials as an Emerging Platform for Theranostics, Mater. Horiz. 6 (2019) 434–469.

[21] R. K. Singh, K. D. Patel, K. W. Leong, H.-W. Kim, Progress in Nanotheranostics Based on Mesoporous Silica Nanomaterial Platforms, ACS Appl. Mater. Interfaces 9 (2017) 10309–10337.

[22] Y. Qiao, J. Wan, L. Zhou, W. Ma, Y. Yang, W. Luo, Z. Yu, H. Wang, Stimuli-responsive nanotherapeutics for precision drug delivery and cancer therapy, Wiley Interdiscip. Rev. Nanomed. Nanobiotechnol. 11 (2019) e1527.

[23] T. L. M. Ten Hagen, M. R. Dreher, S. Zalba, A. L. B. Seynhaeve, M. Amin, L. Li, D. Haemmerich, Drug transport kinetics of intravascular triggered drug delivery systems, Commun. Biol. 4 (2021) 920.

[24] D. J. Phillips, M. I. Gibson, Redox-sensitive materials for drug delivery: targeting the correct intracellular environment, tuning release rates, and appropriate predictive systems, Antioxid. Redox Signal. 21 (2014) 786-803.

[25] D. Rosenblum, N. Joshi, W. Tao, J. M. Karp, D. Peer, Progress and challenges towards targeted delivery of cancer therapeutics, Nat. Commun. 9 (2018) 1410.

[26] R. Baghban, L. Roshangar, R. Jahanban-Esfahlan, K. Seidi, A. Ebrahimi-Kalan, M. Jaymand, S. Kolahian, T. Javaheri, P. Zare, Tumour microenvironment complexity and therapeutic implications at a glance, Cell Commun. Signal. 18 (2020) 59.

[27] G. R. Bhat, I. Sethi, H. Q. Sadida, B. Rah, R. Mir, N. Algehainy, I. A. Albalawi, T. Masoodi, G. K. Subbaraj, F. Jamal, M. Singh, R. Kumar, M. A. Macha, S. Uddin, A. S. A. Akil, M. Haris, A. A. Bhat, Cancer cell plasticity: from cellular, molecular, and genetic mechanisms to tumour heterogeneity and drug resistance, Cancer Metastasis Rev. 43 (2024) 197-228.

[28] M. Riboldi, R. Orecchia, G. Baroni, Real-time tumour tracking in particle therapy: technological developments and future perspectives, Lancet Oncol. 13 (2012) e383-391.

[29] L. Yang, H. Hou, J. Li, Frontiers in fluorescence imaging: tools for the in situ sensing of disease biomarkers, J. Mater. Chem. B 13 (2025) 1133-1158.

[30] F. Stuker, J. Ripoll, M. Rudin, Fluorescence molecular tomography: principles and potential for pharmaceutical research, Pharmaceutics 3 (2011) 229-274.

[31] Y. Luo, L. Huang, Y. Yang, X. Zhuang, S. Hu, H. Ju, B.-Y. Yu, J. Tian, A Programmed Nanoparticle with Self-Adapting for Accurate Cancer Cell Eradication and Therapeutic Self-Reporting, Theranostics 7 (2017) 1245-1256.

[32] A. Sharma, P. Verwilst, M. Li, D. Ma, N. Singh, J. Yoo, Y. Kim, Y. Yang, J. H. Zhu, H. Huang, X. L. Hu, X. P. He, L. Zeng, T. D. James, X. Peng, J. L. Sessler, J. S. Kim, Theranostic Fluorescent Probes, Chem. Rev. 124 (2024) 2699-2804.

[33] K. C. Chong, B. Liu, Reactivity-Based Organic Theranostic Bioprobes, Acc. Chem. Res. 52 (2019) 3051-3063.

[34] Y. Yang, N. Li, Y. Zhu, J. Li, S. Li, X. Hou, Ratiometric singlet oxygen self-detecting and oxygen self-supplying nanosensor for real-time photodynamic therapy feedback and therapeutic effect enhancement, Talanta 259 (2023) 124493.

[35] L. Yang, Q. Chen, S. Gan, C. Huang, H. Zhang, H. Sun, Rational Design of Self-Reporting Photosensitizers for Cell Membrane-Targeted Photodynamic Therapy, Anal. Chem. 95 (2023) 11988-11996.

[36] B. L. Zhang, J. P. Wang, J. Y. Sun, Y. H. Wang, T. M. Chou, Q. Zhang, H. R. Shah, L. Ren, H. J. Wang, Self-Reporting Gold Nanourchins for Tumour-Targeted Chemo-Photothermal Therapy Integrated with Multimodal Imaging, Adv. Ther. 3 (2020) 2000114.

[37] J. Sun, X. W. He, AIE-based drug/gene delivery system: Evolution from fluorescence monitoring alone to augmented therapeutics, Aggregate 3 (2022) e282.

[38] S. Wang, Q. Fu, L. Su, Y. Wu, K. Zhu, D. C. Yang, X. Z. Yang, X. L. Weng, J. Y. Liu, J. Song, Self-Reporting Molecular Prodrug for In Situ Quantitative Sensing of Drug Release by Ratiometric Photoacoustic Imaging, ACS Sens. 8 (2023) 4737-4746.

[39] F. Zheng, W. Xiong, S. Sun, P. Zhang, J. J. Zhu, Recent advances in drug release monitoring, Nanophotonics 8 (2019) 391-413.

[40] Q. Yu, Y. Duan, N. Liu, Z. Zhu, Y. Sun, H. Yang, Y. Shi, X. Li, W. H. Zhu, L. Wang, Q. Wang, Fluorescence and photoacoustic (FL/PA) dual-modal probe: Responsive to reactive oxygen species (ROS) for atherosclerotic plaque imaging, Biomaterials 313 (2025) 122765.

[41] Y. N. Tao, C. X. Yan, Y. Wu, D. Li, J. Li, Y. C. Xie, Y. S. Cheng, Y. S. Xu, K. Yang, W. H. Zhu, Z. Q. Guo, Uniting Dual-Modal MRI/Chemiluminescence Nanotheranostics: Spatially and Sensitively Self-Reporting Photodynamic Therapy in Oral Cancer, Adv. Funct. Mater. 33 (2023) 2303240.



[42] B. Brito, T. W. Price, J. Gallo, M. Bañobre-López, G. J. Stasiuk, Smart magnetic resonance imaging-based theranostics for cancer, Theranostics 11 (2021) 8706-8737.

[43] Y. Zhang, C. Wei, F. Lv, T. Liu, Real-time imaging tracking of a dual-fluorescent drug delivery system based on doxorubicin-loaded globin-polyethylenimine nanoparticles for visible tumour therapy, Colloids Surf. B Biointerfaces 170 (2018) 163-171.

[44] X. Kong, B. Dong, X. Song, C. Wang, N. Zhang, W. Lin, Dual turn-on fluorescence signal-based controlled release system for real-time monitoring of drug release dynamics in living cells and tumour tissues, Theranostics 8 (2018) 800-811.

[45] M. H. Lee, A. Sharma, M. J. Chang, J. Lee, S. Son, J. L. Sessler, C. Kang, J. S. Kim, Fluorogenic reaction-based prodrug conjugates as targeted cancer theranostics, Chem. Soc. Rev. 47 (2018) 28-52.

[46] P. Gong, L. Zhang, J. Peng, S. Li, J. Chen, X. Liu, H. Peng, Z. Liu, J. You, Smart "on-off-on" fluorescent switches for drug visual loading and responsive delivery, Dyes Pigments 173 (2020) 107893.

[47] A. Attri, D. Thakur, T. Kaur, S. Sensale, Z. Peng, D. Kumar, R. P. Singh, Nanoparticles Incorporating a Fluorescence Turn-on Reporter for Real-Time Drug Release Monitoring, a Chemoenhancer and a Stealth Agent: Poseidon's Trident against Cancer? Mol. Pharm. 18 (2021) 124-147.

[48] P. Jirvankar, S. Agrawal, N. Chambhare, R. Agrawal, Harnessing Biopolymer Gels for Theranostic Applications: Imaging Agent Integration and Real-Time Monitoring of Drug Delivery, Gels 10 (2024) 535.

[49] Y. C. Li, Q. H. Chen, X. Y. Pan, W. Lu, J. Zhang, New insight into the application of fluorescence platforms in tumour diagnosis: From chemical basis to clinical application, Med. Res. Rev. 43 (2023) 570-613.

[50] W. L. Li, H. Xin, Y. N. Zhang, C. Feng, Q. D. Li, D. X. Kong, Z. F. Sun, Z. W. Xu, J. M. Xiao, G. Tian, G. L. Zhang, L. Liu, NIR-II Fluorescence Imaging-Guided Oxygen Self-Sufficient Nano-Platform for Precise Enhanced Photodynamic Therapy, Small 18 (2022) e2205647.

[51] X. Q. Kong, B. L. Dong, X. Z. Song, C. Wang, N. Zhang, W. Y. Lin, Dual turn-on fluorescence signal-based controlled release system for real-time monitoring of drug release dynamics in living cells and tumour tissues, Theranostics 8 (2018) 800-811.

[52] A. Hak, V. Ravasaheb Shinde, A. K. Rengan, A review of advanced nanoformulations in phototherapy for cancer therapeutics, Photodiagnosis Photodyn. Ther. 33 (2021) 102205.

[53] A.-G. Niculescu, A. M. Grumezescu, Photodynamic Therapy—An Up-to-Date Review, Appl. Sci. 11 (2021) 3626.

[54] J. Karges, Clinical Development of Metal Complexes as Photosensitizers for Photodynamic Therapy of Cancer, Angew. Chem. Int. Ed. 61 (2022) e202112236.

[55] X. Zhao, J. Liu, J. Fan, H. Chao, X. Peng, Recent progress in photosensitizers for overcoming the challenges of photodynamic therapy: from molecular design to application, Chem. Soc. Rev. 50 (2021) 4185-4219.

[56] X. Xiong, J. Liu, L. Wu, S. Xiong, W. Jiang, P. Wang, Self-assembly strategies of organic small-molecule photosensitizers for photodynamic therapy, Coord. Chem. Rev. 510 (2024) 215863.

[57] M. Lan, S. Zhao, W. Liu, C. S. Lee, W. Zhang, P. Wang, Photosensitizers for Photodynamic Therapy, Adv. Healthc. Mater. 8 (2019) e1900132.

[58] P. Wang, F. Zhou, K. Guan, Y. Wang, X. Fu, Y. Yang, X. Yin, G. Song, X. B. Zhang, W. Tan. In vivo therapeutic response monitoring by a self-reporting upconverting covalent organic framework nanoplatform, Chem. Sci. 11 (2019) 1299-1306.

[59] C. Wang, Y. Sun, S. Huang, Z. Wei, J. Tan, C. Wu, Q. Chen, X. Zhang, Self-Immolative Photosensitizers for Self-Reported Cancer Phototheranostics, J. Am. Chem. Soc. 145 (2023) 13099-13113.

[60] S. Li, F. Yang, Y. Wang, L. Jia, X. Hou, Self-reported and self-facilitated theranostic oxygen nano-economizer for precise and hypoxia alleviation-potentiated photodynamic therapy, Mater. Horiz. 10 (2023) 5734-5752.

[61] Y. Chen, T. Xiong, Q. Peng, J. Du, W. Sun, J. Fan, X. Peng, Self-reporting photodynamic nanobody conjugate for precise and sustainable large-volume tumour treatment, Nat. Commun. 15 (2024) 6935.

[62] M. Xie, T. Gong, Y. Wang, Z. Li, M. Lu, Y. Luo, L. Min, C. Tu, X. Zhang, Q. Zeng, Y. Zhou, Advancements in Photothermal Therapy Using Near-Infrared Light for Bone Tumours, Int. J. Mol. Sci. 25 (2024) 4139. https://doi.org/10.3390/ijms25084139

[63] X. Huang, W. Zhang, G. Guan, G. Song, R. Zou, J. Hu, Design and Functionalization of the NIR-Responsive Photothermal Semiconductor Nanomaterials for Cancer Theranostics, Acc. Chem. Res. 50 (2017) 2529-2538.

[64] C. Li, Y. Cheng, D. Li, Q. An, W. Zhang, Y. Zhang, Y. Fu, Antitumour Applications of Photothermal Agents and Photothermal Synergistic Therapies, Int. J. Mol. Sci. 23 (2022) 7909.

[65] K. F. Chu, D. E. Dupuy, Thermal ablation of tumours: biological mechanisms and advances in therapy, Nat. Rev. Cancer 14 (2014) 199-208.

[66] G. Hannon, F. L. Tansi, I. Hilger, A. Prina-Mello, The Effects of Localized Heat on the Hallmarks of Cancer, Adv. Ther. 4 (2021) 2000294.
[67] X. Sun, J. Sun, B. Dong, G. Huang, L. Zhang, W. Zhou, J. Lv, X. Zhang, M. Liu, L. Xu, X. Bai, W. Xu, Y. Yang, X. Song, H. Song, Noninvasive temperature monitoring for dual-modal tumour therapy based on lanthanide-doped up-conversion nanocomposites, Biomaterials 201 (2019) 42-52.
[68] M. Karimi, P. Sahandi Zangabad, A. Ghasemi, M. Amiri, M. Bahrami, H. Malekzad, H. Ghahramanzadeh Asl, Z. Mahdieh, M. Bozorgomid, A. Ghasemi, M. R. Rahmani Taji Boyuk, M. R. Hamblin, Temperature-Responsive Smart Nanocarriers for Delivery of Therapeutic Agents: Applications and Recent Advances, ACS Appl. Mater. Interfaces 8 (2016) 21107-21133.
[69] M. Overchuk, R. A. Weersink, B. C. Wilson, G. Zheng, Photodynamic and Photothermal Therapies: Synergy Opportunities for Nanomedicine, ACS Nano 17 (2023) 7979-8003.
[70] J. Qiao, X. Mu, L. Qi, Construction of fluorescent polymeric nano-thermometers for intracellular temperature imaging: A review, Biosens. Bioelectron. 85 (2016) 403-413.
[71] G. Feng, H. Zhang, X. Zhu, J. Zhang, J. Fang, Fluorescence thermometers: intermediation of fundamental temperature and light, Biomater. Sci. 10 (2022) 1855-1882.
[72] X. Wu, L. Mu, M. Chen, S. Liang, Y. Wang, G. She, W. Shi, Bifunctional Gold Nanobipyramids for Photothermal Therapy and Temperature Monitoring, ACS Appl. Bio Mater. 2 (2019) 2668-2675.
[73] X. H. Wang, X. Q. Chen, H. S. Peng, X. F. Wei, X. J. Wang, K. Cheng, Y. A. Liu, W. Yang, Facile synthesis of polypyrrole-rhodamine B nanoparticles for self-monitored photothermal therapy of cancer cells, J. Mater. Chem. B 8 (2020) 1033-1039.
[74] L. L. Ma, Y. L. Zhou, Z. W. B. Zhang, Y. Q. Liu, D. Zhai, H. Zhuang, Q. Li, J. D. Yuye, C. T. Wu, J. Chang, Multifunctional bioactive Nd-Ca-Si glasses for fluorescence thermometry, photothermal therapy, and burn tissue repair, Sci. Adv. 6 (2020) eabc5963.
[75] G. Liu, Z. Wang, W. Sun, X. Lin, R. Wang, C. Li, L. Zong, Z. Fu, H. Liu, S. Xu, Robust emission in near-infrared II of lanthanide nanoprobes conjugated with Au (LNPs-Au) for temperature sensing and controlled photothermal therapy, Chem. Eng. J. 452 (2023) 139345. https://doi.org/10.1016/j.cej.2022.139504
[76] Z. Sun, T. Li, F. Wu, T. Yao, H. Yang, X. Yang, H. Yin, Y. Gao, Y. Zhang, C. Li, Q. Wang, Precise Synergistic Photothermal Therapy Guided by Accurate Temperature-Dependent NIR-II Fluorescence Imaging, Adv. Funct. Mater. 34 (2023) 2304144.
[77] S. Y. Qin, A. Q. Zhang, X. Z. Zhang, Recent Advances in Targeted Tumour Chemotherapy Based on Smart Nanomedicines, Small 14 (2018) e1802417.
[78] I. Larionova, N. Cherdyntseva, T. Liu, M. Patysheva, M. Rakina, J. Kzhyshkowska, Interaction of tumour-associated macrophages and cancer chemotherapy, Oncoimmunology 8 (2019) 1596004.
[79] C. M. Tilsed, S. A. Fisher, A. K. Nowak, R. A. Lake, W. J. Lesterhuis, Cancer chemotherapy: insights into cellular and tumour microenvironmental mechanisms of action, Front. Oncol. 12 (2022) 960317.
[80] W. M. C. van den Boogaard, D. S. J. Komninos, W. P. Vermeij, Chemotherapy Side-Effects: Not All DNA Damage Is Equal, Cancers (Basel) 14 (2022) 627.
[81] N. Behranvand, F. Nasri, R. Zolfaghari Emameh, P. Khani, A. Hosseini, J. Garssen, R. Falak, Chemotherapy: a double-edged sword in cancer treatment, Cancer Immunol. Immunother. 71 (2022) 507-526.
[82] Z. Wang, Y. Duan, Y. Duan, Application of polydopamine in tumour targeted drug delivery system and its drug release behavior, J. Control. Release 290 (2018) 56-74.
[83] C. J. Gil, L. Li, B. Hwang, M. Cadena, A. S. Theus, T. A. Finamore, H. Bauser-Heaton, M. Mahmoudi, R. K. Roeder, V. Serpooshan, Tissue engineered drug delivery vehicles: Methods to monitor and regulate the release behavior, J. Control. Release 349 (2022) 143-155.
[84] L. Yang, Y. Yang, Y. Chen, Y. Xu, J. Peng, Cell-based drug delivery systems and their in vivo fate, Adv. Drug Deliv. Rev. 187 (2022) 114394.
[85] X. Zhao, Y. Ma, Z. Lei, Advanced optical imaging technology in the near infrared window for cell tracking in vivo, Coord. Chem. Rev. 521 (2024) 215424.
[86] X. Liu, B. Yu, Y. Shen, H. Cong, Design of NIR-II high performance organic small molecule fluorescent probes and summary of their biomedical applications, Coord. Chem. Rev. 468 (2022) 214418.
[87] J. Yao, M. Yang, Y. Duan, Chemistry, biology, and medicine of fluorescent nanomaterials and related systems: new insights into biosensing, bioimaging, genomics, diagnostics, and therapy, Chem. Rev. 114 (2014) 6130-6178.
[88] M. L. Kabir, F. Wang, A. H. A. Clayton, Intrinsically Fluorescent Anti-Cancer Drugs, Biology 11 (2022) 1135. https://doi.org/10.3390/biology11081135
[89] S. Roy, N. Bag, S. Bardhan, I. Hasan, B. Guo, Recent progress in NIR-II fluorescence imaging-guided drug delivery for cancer theranostics, Adv. Drug Deliv. Rev. 197 (2023) 114821.
[90] M. Gao, F. Yu, C. Lv, J. Choo, L. Chen, Fluorescent chemical probes for accurate tumour diagnosis and targeting therapy, Chem. Soc. Rev. 46 (2017) 2237-2271.

[91] Z. Wang, H. Wu, P. Liu, F. Zeng, S. Wu, A self-immolative prodrug nanosystem capable of releasing a drug and a NIR reporter for in vivo imaging and therapy, Biomaterials 139 (2017) 139-150.

[92] M. Zhang, C. C. Song, S. Su, F. S. Du, Z. C. Li, ROS-Activated Ratiometric Fluorescent Polymeric Nanoparticles for Self-Reporting Drug Delivery, ACS Appl. Mater. Interfaces 10 (2018) 7798-7810.

[93] J. Li, Y. J. Wei, X. L. Yang, W. X. Wu, M. Q. Zhang, M. Y. Li, Z. E. Hu, Y. H. Liu, N. Wang, X. Q. Yu, Rational Construction of a Mitochondrial Targeting, Fluorescent Self-Reporting Drug-Delivery Platform for Combined Enhancement of Endogenous ROS Responsiveness, ACS Appl. Mater. Interfaces 12 (2020) 32432-32445.

[94] S. Kayal, P. Kola, J. Pal, M. Mandal, D. Dhara, Self-Indicating Polymer Prodrug Nanoparticles for pH-Responsive Drug Delivery in Cancer Cells and Real-Time Monitoring of Drug Release, ACS Appl. Bio Mater. 7 (2024) 5810-5822.

[95] M. Liu, Y. Li, F. Wang, S. Lu, L. Jiang, X. Chen, Light-triggered release of lenalidomide with fluorescent indication for inhibition of COX-2 enzyme activity in cancer cells, Chem. Commun. (Camb) (2025) 6518-6521.

[96] M. P. Jogalekar, R. L. Rajendran, F. Khan, C. Dmello, P. Gangadaran, B. C. Ahn, CAR T-Cell-Based gene therapy for cancers: new perspectives, challenges, and clinical developments, Front. Immunol. 13 (2022) 925985.

[97] T. M. Belete, The Current Status of Gene Therapy for the Treatment of Cancer, Biologics 15 (2021) 67-77.

[98] N. Qiu, G. Wang, J. Wang, Q. Zhou, M. Guo, Y. Wang, X. Hu, H. Zhou, R. Bai, M. You, Z. Zhang, C. Chen, Y. Liu, Y. Shen, Tumour-Associated Macrophage and Tumour-Cell Dually Transfecting Polyplexes for Efficient Interleukin-12 Cancer Gene Therapy, Adv. Mater. 33 (2021) e2006189.

[99] R. Liu, Y. Peng, L. Lu, S. Peng, T. Chen, M. Zhan, Near-infrared light-triggered nano-prodrug for cancer gas therapy, J. Nanobiotechnol. 19 (2021) 443.

[100] X. Yao, B. Yang, J. Xu, Q. He, W. Yang, Novel gas-based nanomedicines for cancer therapy, View 3 (2022) 1-15.

[101] H. Z. Yang, Y. Guo, L. Pu, X. Q. Yu, J. Zhang, Fluorescent Self-Reporting Lipid Nanoparticles for Nitric Oxide/Gene Co-Delivery and Combination Therapy, Mol. Pharm. 20 (2023) 1404-1414.

[102] S. Yang, J. Luo, L. Zhang, L. Feng, Y. He, X. Gao, S. Xie, M. Gao, D. Luo, K. Chang, M. Chen, A Smart Nano-Theranostic Platform Based on Dual-microRNAs Guided Self-Feedback Tetrahedral Entropy-Driven DNA Circuit, Adv. Sci. 10 (2023) e2301814.

[103] Y. Wu, Y. Song, R. Wang, T. Wang, Molecular mechanisms of tumour resistance to radiotherapy, Mol. Cancer 22 (2023) 96.

[104] H. Chen, Z. Han, Q. Luo, Y. Wang, Q. Li, L. Zhou, H. Zuo, Radiotherapy modulates tumour cell fate decisions: a review, Radiat. Oncol. 17 (2022) 196.

[105] X. Ge, L. Su, Z. Chen, K. Zhu, X. Zhang, Y. Wu, J. Song, A Radio-Pharmaceutical Fluorescent Probe for Synergistic Cancer Radiotherapy and Ratiometric Imaging of Tumour Reactive Oxygen Species, Angew. Chem. Int. Ed. 62 (2023) e202305744.

[106] Fu Q, Wei C, Wang M. Transition-metal-based nanozymes: synthesis, mechanisms of therapeutic action, and applications in cancer treatment[J]. ACS nano, 2024, 18(19): 12049-12095.

[107] Sun D, Sun X, Zhang X, et al. Emerging chemodynamic nanotherapeutics for cancer treatment[J]. Advanced Healthcare Materials, 2024, 13(22): 2400809.

[108] Hao J N, Ge K, Chen G, et al. Strategies to engineer various nanocarrier-based hybrid catalysts for enhanced chemodynamic cancer therapy[J]. Chemical Society Reviews, 2023, 52(22): 7707-7736.

[109] P. Zhao, H. Li, W. Bu, A Forward Vision for Chemodynamic Therapy: Issues and Opportunities, Angew. Chem. Int. Ed. 62 (2023) e202210415.

[110] D. Jana, Y. Zhao, Strategies for enhancing cancer chemodynamic therapy performance, Exploration (Beijing) 2 (2022) 20210238.

[111] Y. Ma, C. Yan, Z. Guo, G. Tan, D. Niu, Y. Li, W. H. Zhu, Spatio-Temporally Reporting Dose-Dependent Chemotherapy via Uniting Dual-Modal MRI/NIR Imaging, Angew. Chem. Int. Ed. 59 (2020) 21143-21150.

[112] M. Yu, Z. Ye, S. Liu, Y. Zhu, X. Niu, J. Wang, R. Ao, H. Huang, H. Cai, Y. Liu, X. Chen, L. Lin, Redox-Active Ferrocene Quencher-Based Supramolecular Nanomedicine for NIR-II Fluorescence-Monitored Chemodynamic Therapy, Angew. Chem. Int. Ed. 63 (2024) e202318155.

[113] D. Li, AIEgen functionalized inorganic–organic hybrid nanomaterials for cancer diagnosis and therapy, Inorg. Chem. Front. 6 (2019) 1613-1622.

[114] M. Wang, S. Bai, Y. Zhang, Single- and multi-modal molecular probes with second near-infrared activatable optical signals for disease diagnosis and theranostics, Chem. Soc. Rev. 54 (2025) 7561-7609.

[115] P. Thapa, V. Singh, S. Bhatt, K. Maurya, V. Kumar, V. Nayyar, K. Jot, D. Mishra, A. Shrivastava, D. S. Mehta, Multimodal fluorescence imaging and spectroscopic techniques for oral cancer screening: a real-time approach, Methods Appl. Fluoresc. 11 (2023) 1-20.

[116] Y. Yang, Q. Jiang, F. Zhang, Nanocrystals for Deep-Tissue In Vivo Luminescence Imaging in the Near-Infrared Region, Chem. Rev. 124 (2024) 554-628.

[117] N. Khemthongcharoen, R. Jolivot, S. Rattanavarin, W. Piyawattanametha, Advances in imaging probes and optical microendoscopic imaging techniques for early in vivo cancer assessment, Adv. Drug Deliv. Rev. 74 (2014) 53-74.
[118] Z. Zheng, R. Dai, Z. Jia, X. Yang, Y. Qin, S. Rong, X. Peng, X. Xie, Y. Wang, R. Zhang, Biodegradable Multifunctional Nanotheranostic Based on Ag(2)S-Doped Hollow BSA-SiO(2) for Enhancing ROS-Feedback Synergistic Antitumour Therapy, ACS Appl. Mater. Interfaces 12 (2020) 54356-54366.
[119] C. Lv, Z. Li, W. Liu, M. Yang, H. Zhang, J. Fan, X. Peng, An Activatable Chemiluminescent Self-Reporting Sulfur Dioxide Donor for Inflammatory Response and Regulation of Gaseous Vasodilation, ACS Sens. 10 (2025) 1147-1154.
[120] Z. Zhang, R. Wang, R. Luo, J. Zhu, X. Huang, W. Liu, F. Liu, F. Feng, W. Qu, An Activatable Theranostic Nanoprobe for Dual-Modal Imaging-Guided Photodynamic Therapy with Self-Reporting of Sensitizer Activation and Therapeutic Effect, ACS Nano 15 (2021) 5366-5383.
[121] C. Lu, C. Zhang, P. Wang, Y. Zhao, Y. Yang, Y. Wang, H. Yuan, S. Qu, X. Zhang, G. Song, K. Pu, Light-free Generation of Singlet Oxygen through Manganese-Thiophene Nanosystems for pH-Responsive Chemiluminescence Imaging and Tumour Therapy, Chem 6 (2020) 2314-2334.
[122] M. Wang, W. Liu, B. Li, W. Zhu, D. Li, J. Li, Z. Hai, An Integrative Probe for Tumour Therapy and Dual-Modal Self-Evaluation Imaging of Therapeutic Efficacy, ACS Mater. Lett. 6 (2024) 4617-4623.
[123] H. Liu, Y. Guo, J. Lv, J. Xu, Q. Zhang, G. Guan, C. Zhang, C. Lu, Q. Gong, C. Liang, D. Xu, G. Song, Enhanced Real-Time Monitoring of Catalytic Therapy Efficacy with Dual-Channel MRI and Fluorescent Platform, Adv. Funct. Mater. 35 (2025) 2412848.
[124] J. J. M. Riksen, A. V. Nikolaev, G. van Soest, Photoacoustic imaging on its way toward clinical utility: a tutorial review focusing on practical application in medicine, J. Biomed. Opt. 28 (2023) 121205.
[125] H. Liu, X. Teng, S. Yu, W. Yang, T. Kong, T. Liu, Recent Advances in Photoacoustic Imaging: Current Status and Future Perspectives, Micromachines (Basel) 15 (2024) 1-25.
[126] W. Choi, B. Park, S. Choi, D. Oh, J. Kim, C. Kim, Recent Advances in Contrast-Enhanced Photoacoustic Imaging: Overcoming the Physical and Practical Challenges, Chem. Rev. 123 (2023) 7379-7419.
[127] L. Lin, L. V. Wang, The emerging role of photoacoustic imaging in clinical oncology, Nat. Rev. Clin. Oncol. 19 (2022) 365-384.
[128] Q. Fu, R. Zhu, J. Song, H. Yang, X. Chen, Photoacoustic Imaging: Contrast Agents and Their Biomedical Applications, Adv. Mater. 31 (2019) e1805875.
[129] N. Kwon, K. H. Kim, S. Park, Y. Cho, E. Y. Park, J. Lim, S. Cetindere, S. O. Tumay, W. J. Kim, X. Li, K. T. Nam, C. Kim, S. Yesilot, J. Yoon, Hexa-BODIPY-cyclotriphosphazene based nanoparticle for NIR fluorescence/photoacoustic dual-modal imaging and photothermal cancer therapy, Biosens. Bioelectron. 216 (2022) 114612.
[130] Z. Fan, X. Jiang, T. Sun, F. Zeng, G. Huang, C. Liang, L. Nie, In vivo visualization of tumour-associated macrophages re-education by photoacoustic/fluorescence dual-modal imaging with a metal-organic frames-based caspase-1 nanoreporter, J. Colloid Interface Sci. 659 (2024) 48-59.
[131] M. Yang, J. Huang, J. Fan, J. Du, K. Pu, X. Peng, Chemiluminescence for bioimaging and therapeutics: recent advances and challenges, Chem. Soc. Rev. 49 (2020) 6800-6815.
[132] H. Shen, F. Sun, X. Zhu, J. Zhang, X. Ou, J. Zhang, C. Xu, H. H. Y. Sung, I. D. Williams, S. Chen, R. T. K. Kwok, J. W. Y. Lam, J. Sun, F. Zhang, B. Z. Tang, Rational Design of NIR-II AIEgens with Ultrahigh Quantum Yields for Photo- and Chemiluminescence Imaging, J. Am. Chem. Soc. 144 (2022) 15391-15402.
[133] R. Blau, O. Shelef, D. Shabat, R. Satchi-Fainaro, Chemiluminescent probes in cancer biology, Nat. Rev. Bioeng. 1 (2023) 648-664.
[134] X. Dong, L. Sun, Z. Zhang, T. Zhu, J. Sun, J. Gao, C. Dong, R. Wang, X. Gu, C. Zhao, A dual-modality hydrogen sulfide-specific probe integrating chemiluminescence with NIR fluorescence for targeted cancer imaging, Sci. China Chem. 66 (2023) 1869-1876.
[135] Y. Tao, C. Yan, Y. Wu, D. Li, J. Li, Y. Xie, Y. Cheng, Y. Xu, K. Yang, W. H. Zhu, Z. Guo, Uniting Dual-Modal MRI/Chemiluminescence Nanotheranostics: Spatially and Sensitively Self-Reporting Photodynamic Therapy in Oral Cancer, Adv. Funct. Mater. 33 (2023) 2300644.
[136] Q. R. Fu, Harnessing Biomarker Activatable Probes for Early Stratification and Timely Assessment of Therapeutic Efficacy in Cancer, Exploration-Prc 5 (2025) 1-20.
[137] J. Niu, F. Meng, Q. Hao, J. Fu, C. Zong, M. Tian, X. Yu, A self-reporting photosensitizer for inducing and in-situ monitoring lysosomal damage and cell apoptosis, Sens. Actuators B Chem. 382 (2023) 133568.
[138] T. Zhang, Y. Li, Z. Zheng, R. Ye, Y. Zhang, R. T. K. Kwok, J. W. Y. Lam, B. Z. Tang, In Situ Monitoring Apoptosis Process by a Self-Reporting Photosensitizer, J. Am. Chem. Soc. 141 (2019) 5612-5616.

[139] S. Zeng, X. Liu, Y. S. Kafuti, H. Kim, J. Wang, X. Peng, H. Li, J. Yoon, Fluorescent dyes based on rhodamine derivatives for bioimaging and therapeutics: recent progress, challenges, and prospects, Chem. Soc. Rev. 52 (2023) 5607-5651.

[140] Y. Yuan, C. J. Zhang, R. T. K. Kwok, S. Xu, R. Zhang, J. Wu, B. Z. Tang, B. Liu, Light-Up Probe for Targeted and Activatable Photodynamic Therapy with Real-Time in Situ Reporting of Sensitizer Activation and Therapeutic Responses, Adv. Funct. Mater. 25 (2015) 6586-6595.

[141] X. Zhang, W. Chen, X. Xie, Y. Zhang, Z. Chao, H. Ma, Y. Liu, H. Ju, Energy Pumping by Surface Collectors on Upconversion Nanoparticles for Extended Transfer and Efficient Self-Evaluable Photodynamic Therapy, CCS Chem. 4 (2022) 1251-1262.

[142] D. H. Wang, L. J. Chen, X. Zhao, X. P. Yan, A unique self-reporting photosensitizer enabling simultaneous photodynamic therapy and real-time monitoring of phototheranostic process in a dynamic dual-color mode, J. Mater. Chem. B 9 (2021) 9900-9907.

[143] L. Peng, W. Chen, H. Hou, M. Tian, F. Song, W.-H. Zheng, X. Peng, Red-to-near-infrared self-reporting photosensitizers with high photostability for photodynamic therapy, Dyes Pigments 217 (2023) 111345.

[144] Y. Xu, J. Zhang, Z. Wang, P. Zhang, Z. Zhang, Z. Yang, J. W. Y. Lam, R. T. K. Kwok, L. Meng, D. Dang, B. Z. Tang, Water-soluble AIE photosensitizer in short-wave infrared region for albumin-enhanced and self-reporting phototheranostics, Biomaterials 314 (2025) 122847.

[145] R. Zhang, C. Zhang, Q. Lu, C. Liang, M. Tian, Z. Li, Y. Yang, X. Li, Y. Deng, Cancer-cell-specific Self-Reporting Photosensitizer for Precise Identification and Ablation of Cancer Cells, Anal. Chem. 96 (2024) 1659-1667.

[146] W. Bian, Q. Wang, C. He, P. Tao, J. Zheng, Y. Zhang, J. Li, F. Li, H. Jia, D. Ling, A Real-Time Cell Death Self-Reporting Theranostic Agent for Dynamic Optimization of Photodynamic Therapy, Adv. Sci. (Weinh) (2025) 2417678

[147] P. Yin, Z. An, J. Han, R. Zhang, J. Jing, X. Zhang, Mitochondrial-targeted type I/II self-reporting photosensitizer with viscosity-sensitive properties for tumour recognition and apoptosis induction, Sens. Actuators B Chem. 447 (2026) 130945.

[148] Y. Wang, W. Du, T. Zhang, Y. Zhu, Y. Ni, C. Wang, F. M. Sierra Raya, L. Zou, L. Wang, G. Liang, A Self-Evaluating Photothermal Therapeutic Nanoparticle, ACS Nano 14 (2020) 9585-9593.

[149] L. Liu, X. Li, H. Zhang, H. Chen, M. M. A. Abualrejal, D. Song, Z. Wang, Six-in-one peptide functionalized upconversion@polydopamine nanoparticle-based ratiometric fluorescence sensing platform for real-time evaluating anticancer efficacy through monitoring caspase-3 activity, Sens. Actuators B Chem. 333 (2021) 129533.

[150] Z. Long, J.-J. Hu, L. Yuan, C. Duan, J. Dai, S. Zhen, Z. Zhao, X. Lou, F. Xia, A cell membrane-anchored nanoassembly with self-reporting property for enhanced second near-infrared photothermal therapy, Nano Today 41 (2021) 101264.

[151] B. Li, H. Liu, Y. He, M. Zhao, C. Ge, M. R. Younis, P. Huang, X. Chen, J. Lin, A "Self-Checking" pH/Viscosity-Activatable NIR-II Molecule for Real-Time Evaluation of Photothermal Therapy Efficacy, Angew. Chem. Int. Ed. 61 (2022) e202200025.

[152] J. Shi, O. Alagoz, F. S. Erenay, Q. Su, A survey of optimization models on cancer chemotherapy treatment planning, Ann. Oper. Res. 221 (2011) 331-356.

[153] J. Tian, Y. Luo, L. Huang, Y. Feng, H. Ju, B.-Y. Yu, Pegylated folate and peptide-decorated graphene oxide nanovehicle for in vivo targeted delivery of anticancer drugs and therapeutic self-monitoring, Biosens. Bioelectron. 80 (2016) 519-524.

[154] Y. Luo, L. Huang, Y. Yang, X. Zhuang, S. Hu, H. Ju, B. Y. Yu, J. Tian, A Programmed Nanoparticle with Self-Adapting for Accurate Cancer Cell Eradication and Therapeutic Self-Reporting, Theranostics 7 (2017) 1245-1256.

[155] Y. Yang, Y. He, Z. Deng, J. Li, J. Huang, S. Zhong, Intelligent Nanoprobe: Acid-Responsive Drug Release and In Situ Evaluation of Its Own Therapeutic Effect, Anal. Chem. 92 (2020) 12371-12378.

[156] S. Pei, Z. Liu, Q. Jiao, Q. Jin, X. Luo, Y. Liu, S. Zhou, S. Pang, X. Wu, K. Xu, W. Zhong, Self-Reporting Ratiometric AIEgen-Peptide Nanoprobes for Activatable Chemotherapy and Noninvasive Imaging of Therapeutic Outcomes, J. Med. Chem. 68 (2025) 7767-7779.

[157] L. Wang, W. Jiang, L. Xiao, H. Li, Z. Chen, Y. Liu, J. Dou, S. Li, Q. Wang, W. Han, Y. Wang, H. Liu, Self-Reporting and Splitting Nanopomegranates Potentiate Deep Tissue Cancer Radiotherapy via Elevated Diffusion and Transcytosis, ACS Nano 14 (2020) 8459-8472.

[158] L. Yue, K. Yang, J. Li, Q. Cheng, R. Wang, Self-Propelled Asymmetrical Nanomotor for Self-Reported Gas Therapy, Small 17 (2021) e2102286.

[159] S. Zhang, Y. Zhang, Y. Feng, J. Wu, Y. Hu, L. Lin, C. Xu, J. Chen, Z. Tang, H. Tian, X. Chen, Biomineralized Two-Enzyme Nanoparticles Regulate Tumour Glycometabolism Inducing Tumour Cell Pyroptosis and Robust Antitumour Immunotherapy, Adv. Mater. 34 (2022) e2206851.

[160] V. Salemme, G. Centonze, F. Cavallo, P. Defilippi, L. Conti, The Crosstalk Between Tumour Cells and

the Immune Microenvironment in Breast Cancer: Implications for Immunotherapy, Front. Oncol. 11 (2021) 610303.
[161] M. Zhang, X. Jin, M. Gao, Y. Zhang, B. Z. Tang, A Self-Reporting Fluorescent Salicylaldehyde-Chlorambucil Conjugate as a Type-II ICD Inducer for Cancer Vaccines, Adv. Mater. 34 (2022) e2205701.
[162] J. Yang, A. Griffin, Z. Qiang, J. Ren, Organelle-Targeted Therapies: A Comprehensive Review on System Design for Enabling Precision Oncology, Signal Transduct. Target. Ther. 7 (2022) 379.
[163] W.-H. Chen, G.-F. Luo, X.-Z. Zhang, Recent Advances in Subcellular Targeted Cancer Therapy Based on Stimuli-Responsive Nanomaterials, Adv. Mater. 31 (2019) 1802725.
[164] W. Zhen, S. An, S. Wang, W. Hu, Y. Li, X. Jiang, J. Li, Precise Subcellular Organelle Targeting for Boosting Endogenous-Stimuli-Mediated Tumor Therapy, Adv. Mater. 33 (2021) 2101572
[165] B. Chen, J. J. Hu, H. Ouyang, W. Zhang, J. Dai, L. Xu, F. Xia, X. Lou, Peptide-Conjugated Probe Inducing Mitochondrial Dysfunction and Self-Reporting Cell Apoptosis by Aggregated Proteins, Anal. Chem. 95 (2023) 12903-12912.
[166] M. Xu, Y. Hu, J. Wu, J. Liu, K. Pu, Sonodynamic Nano-LYTACs Reverse Tumour Immunosuppressive Microenvironment for Cancer Immunotherapy, J. Am. Chem. Soc. 146 (2024) 34669-34680.
[167] M. Bekes, D. R. Langley, C. M. Crews, PROTAC targeted protein degraders: the past is prologue, Nat. Rev. Drug Discov. 21 (2022) 181-200.
[168] C. Zhang, Z. Zeng, D. Cui, S. He, Y. Jiang, J. Li, J. Huang, K. Pu, Semiconducting polymer nano-PROTACs for activatable photo-immunometabolic cancer therapy, Nat. Commun. 12 (2021) 2934.
[169] X. Teng, X. Zhao, Y. Dai, X. Zhang, Q. Zhang, Y. Wu, D. Hu, J. Li, ClickRNA-PROTAC for Tumour-Selective Protein Degradation and Targeted Cancer Therapy, J. Am. Chem. Soc. 146 (2024) 27382-27391.
[170] W. Zhang, L. Yuan, R. Liu, Y. Jing, S. Lin, H. Fang, Y. Li, X. Zhang, J. Dai, T. Liu, F. Xia, X. Lou, A Covalent Self-Reporting Peptide Degrader Enables Real-Time Monitoring of Targeted Protein Degradation In Vivo, J. Am. Chem. Soc. 147 (2025) 27862-27875.
[171] F. Sun, T. Wang, P. Wang, J. Shi, Y. Shen, G. Wang, B. Yang, H. Li, Q. Zhang, Y. Chen, X. Zhang, A Versatile Bioorthogonal Theranostic Platform Enables Relay Activation of Tumour Cell Imaging and Targeted Protein Degradation, J. Am. Chem. Soc. 148 (2026) 258–268.
[172] F. Bruno, V. Granata, F. C. Bellisari, F. Sgalambro, E. Tommasino, P. Palumbo, F. Arrigoni, D. Cozzi, F. Grassi, M. C. Brunese, S. Pradella, M. L. M. D. Stefano, C. Cutolo, E. Di Cesare, A. Splendiani, A. Giovagnoni, V. Miele, R. Grassi, C. Masciocchi, A. Barile, Advanced Magnetic Resonance Imaging (MRI) Techniques: Technical Principles and Applications in Nanomedicine, Cancers 14 (2022) 1-32.
[173] S. Wang, W. Liu, Y. Cao, J. Wang, K. Zhu, Z. Li, J. Cao, C. Mo, Q. Chen, W. Huang, Y. Wu, L. Chen, J. Song, Janus Nanoprobe with Dual-Modal NIR-II Fluorescence/Photoacoustic Imaging for Precision Cancer Radiosensitizing Therapy, ACS Appl. Mater. Interfaces 17 (2025) 29266-29275.
[174] X. Xiao, H. Cai, Q. Huang, B. Wang, X. Wang, Q. Luo, Y. Li, H. Zhang, Q. Gong, X. Ma, Z. Gu, K. Luo, Polymeric dual-modal imaging nanoprobe with two-photon aggregation-induced emission for fluorescence imaging and gadolinium-chelation for magnetic resonance imaging, Bioact. Mater. 19 (2023) 538-549.
[175] M. Zhou, L. Li, W. Xie, Z. He, J. Li, Synthesis of a Thermal-Responsive Dual-Modal Supramolecular Probe for Magnetic Resonance Imaging and Fluorescence Imaging, Macromol. Rapid Commun. 42 (2021) e2100248.
[176] X. Nan, J. Zuo, L. He, Z. Liu, T. Wang, P. Bai, Application of magnetic targeted fluorescence/magnetic resonance dual-modal imaging in cancer diagnosis, J. Nanopart. Res. 25 (2023) 1-18.

View Article Online
DOI: 10.1039/D5TC04393J

The data supporting this article have been included as part of the Supplementary Information.

Supplementary information: Additional TEM, SEM, temperature PL and TRPL data (Fig. S1, Fig. S2, Fig. S3, and Table S1.)